LIGO Laboratory / LIGO Scientific Collaboration

LIGO-L0900118-V8 *LIGO* June 26 , 2009

Advanced LIGO Preliminary Design Review

of the BSC ISI system

F.MATICHARD, B. ABBOTT, S. BARNUM, S. FOLEY, B. LANTZ, K. MASON,
R. MITTLEMAN, C. RAMET, B. O'REILLY, A. STEIN

Distribution of this document:
Advanced LIGO Project

This is an internal working note
of the LIGO Laboratory

California Institute of Technology
LIGO Project – MS 18-34
1200 E. California Blvd.
Pasadena, CA 91125
Phone (626) 395-2129
Fax (626) 304-9834
E-mail: info@ligo.caltech.edu

Massachusetts Institute of Technology
LIGO Project – NW22-295
185 Albany St
Cambridge, MA 02139
Phone (617) 253-4824
Fax (617) 253-7014
E-mail: info@ligo.mit.edu

LIGO Hanford Observatory
P.O. Box 1970
Mail Stop S9-02
Richland WA 99352
Phone 509-372-8106
Fax 509-372-8137

LIGO Livingston Observatory
P.O. Box 940
Livingston, LA 70754
Phone 225-686-3100
Fax 225-686-7189

Contents

1 Introduction

1.1 General Overview

The BSC Internal Seismic Isolation (BSC-ISI) system is a two stage platform that will be installed prior to Advanced LIGO into the BSC chambers. A BSC-ISI system will be installed in each of the 15 BSC chambers. It supports the test masses and beam splitters which are suspended from the triple and quadruple pendulums structures. The BSC-ISI system is shown in Figure 1, installed on the support tubes of the HEPI-BSC. In Figure 2, the BSC-ISI is on its assembly stand at LASTI. A quadruple pendulum is hanging from the optical table.

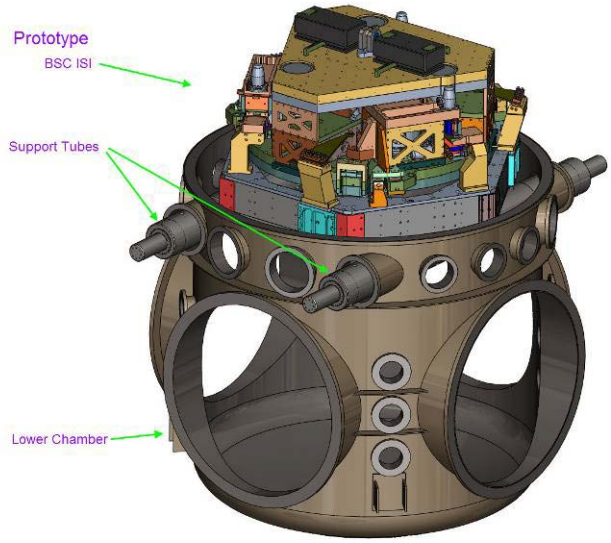

Figure 1

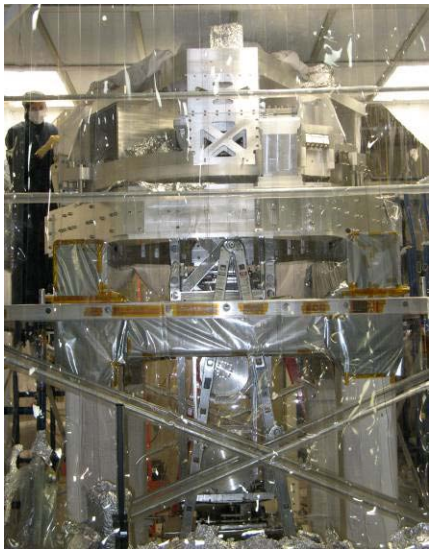

Figure 2

1.2 General Architecture

Both stages are suspended and have 6 degrees of freedom. Stage 0, the base, is represented in violet in Figure 3. It holds Stage 1, represented in cyan, via blades and flexure rods represented in yellow. The blades provide the vertical flexibility; the rods provide the horizontal one. Stage 1 holds Stage 2, represented in grey, via the same type of blades and flexure rods. The suspended stages have natural frequencies in the 1Hz-7Hz range. The system provides passive isolation above its natural frequencies and active control in the 0.1Hz-20Hz range. A detailed description of the system is given in section 2.

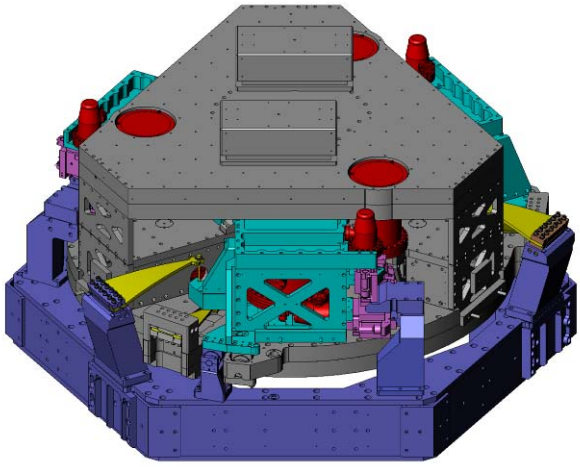

Figure 3

Figure 4

1.3 Active control Isolation

Active isolation is used to provide seismic isolation below 20Hz. Both stages are actively controlled. Six electromagnetic actuators, called large actuators, are used between stage 0 and stage 1. They are shown in pink on Figure 3. Six smaller electromagnetic actuators, called fine actuators, are used between stage 1 and stage 2. The blades, rods and actuators have been positioned to decouple the horizontal and vertical motion of the stages.

Stage 1 is instrumented with three different sets of instruments:

- 6 capacitive position sensors between stage 0 and stage1. They provide the low frequency relative positioning.

- 3 Nanometric Trillium seismometers: these 3 axis seismometers provide the low frequency inertial measurements necessary to provide active seismic isolation.

- 6 Mark Product L4C geophones: those single axis seismometers provide the high frequency inertial positioning necessary to provide active seismic isolation at higher frequencies.

Stage 2 is instrumented with two different sets of instruments:

- 6 capacitive position sensors between stage 0 and stage1. They provide the low frequency relative positioning.

- 6 Geotech GS13 seismometers: those single axis seismometers provide the high frequency inertial positioning necessary to provide active seismic isolation at higher frequencies.

The active control strategy and performance are presented in section 8.

1.4 Background and organization of the document.

The design requirements have been compiled and last updated in May 2004 in the document LIGO-E030179-A, Design Requirements for the In-Vacuum Mechanical Elements of the Advanced LIGO Seismic Isolation System for the BSC Chamber.

The initial design of the BSC-ISI was done by ASI. Their design was presented in the document “Advanced LIGO BSC Prototype Critical Design Review, June 18 2004”. A technical memorandum was delivered on October 15, 2004 and a transition meeting was held on January 18-19, 2005. A critical review has been presented by the SEI team on January 2005, document G050007-00-R. The analysis showed that this design should meet most of the design requirements as described on "Design requirements summary", page 4-10 of “Advanced LIGO BSC Prototype Critical Design Review". The initial design is described in part 2 of this document. Requirements which were not met were waived by the SEI team.

A prototype of the BSC-ISI was then built by Limerick and assembled at MIT in 2006. This first assembly was a dirty one whose purpose was to check the parts fitting and the low frequency motions decoupling. The prototype has then been disassembled, cleaned, reassembled and tested in air. Those steps are described in section 3 of this document.

The system has then been inserted in the BSC chamber. A first control commissioning has been done in summer-fall 2008. This first commissioning showed that the system could be successfully controlled but also highlighted a number of problems that needed to be fixed. They were mostly system resonances too low in frequencies and too numerous. One other major issue was the time-varying characteristics of the system. Those problems have been investigated and solved during the winter-spring 2009. A second round of control commissioning has started after we have closed the

chamber on May 5, 2009. The prototype testing and commissioning are described in part 3, the performance is described in part 8.

These phases of prototyping and testing allowed us to establish a list of changes that were necessary to implement. LIGO engineers have been working since the beginning of 2009 on implementing those changes. They are presented in section 4 of this document.

Sensors and actuators are presented in section 5, the electronics in section 6. Section 7 describes the cleaning, the assembly, the storage and the installation of the system. The performance is presented in section 8. Section 9 lists the current procurement schedule. The work to be done by the FDR is listed in section 10. The last section is the PDR check list defined as required in the LIGO document M050220, Guidelines for Advanced LIGO Detector Construction Activities.

2 Initial design

The BSC-ISI is represented in Figure 5 as built for the prototype installed at LASTI. Figure 6 shows Stage 0 with the Stage0-to-Stage1 lockers and the Blade posts for Stage 1.

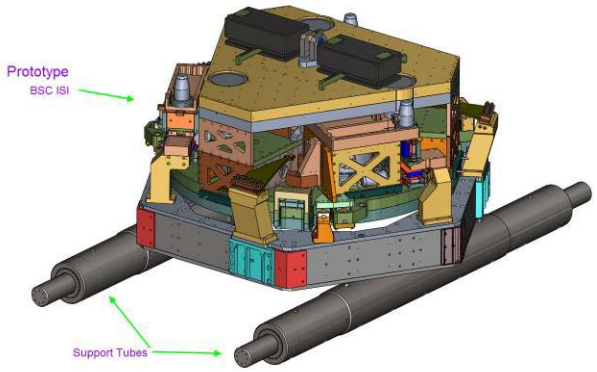

Figure 5

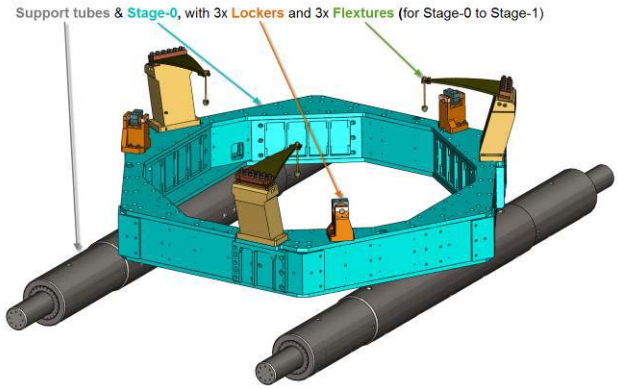

Figure 6

Stage1 is suspended to the flexure rods as shown on figure 7. Stage 1 instruments are not shown in this picture.

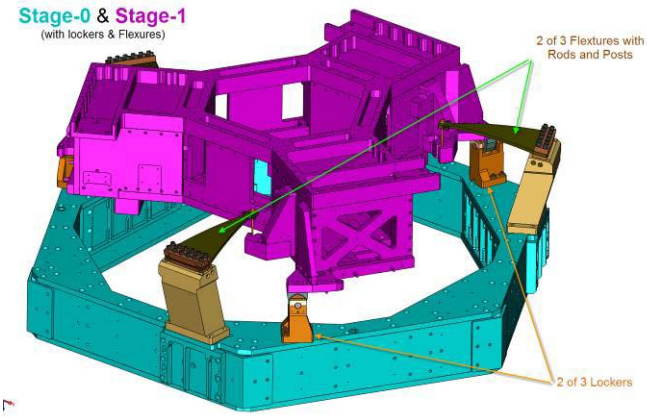

Figure 7

Stage 1 and Stage2 fit together as shown in Figure 8. Figure 9 zooms on the flexure rod connections.

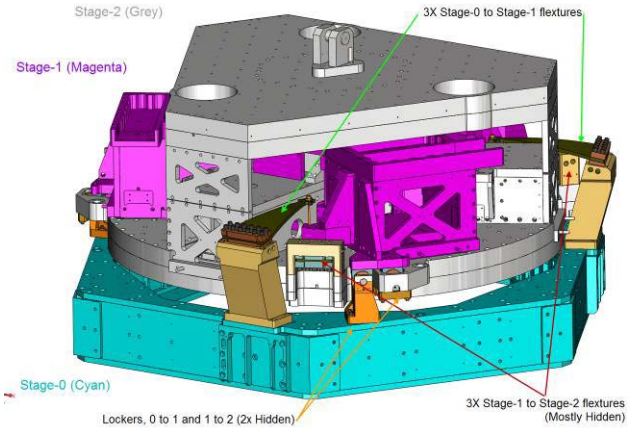

Figure 8

Figure 9

Figure 10 and 11 show the position of the instruments on the stages.

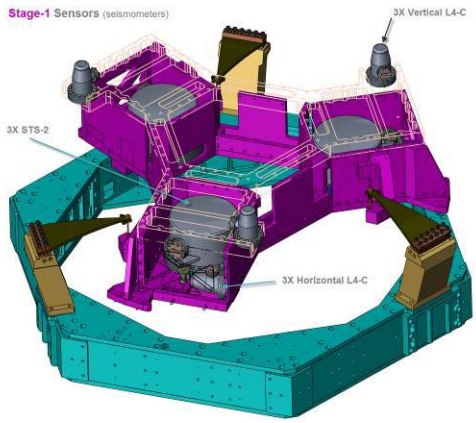

Figure 10

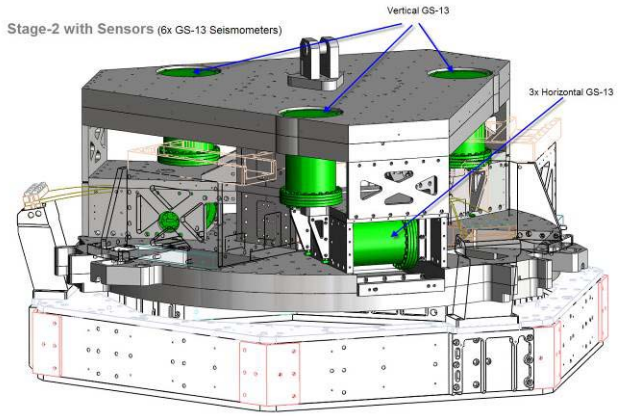

Figure 11

Figure 12 and 13 show the position of the electromagnetic actuators.

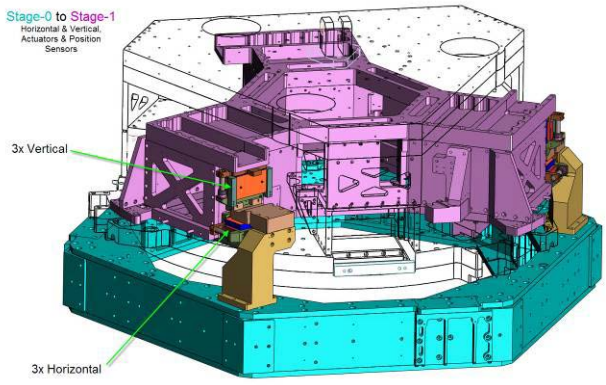

Figure 12

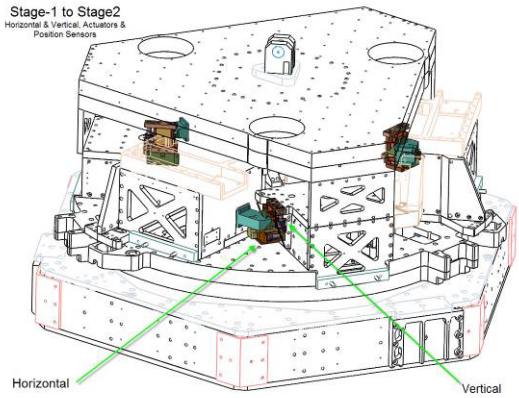

Figure 13

A more detailed description can be found in the document ASI 20008644, “Advanced LIGO BSC Prototype Critical Design Review".

3 Prototype assembly and testing

A prototype of the BSC-ISI has been built and first assembled at MIT in 2006. This section describes this prototyping phases including the successive steps of dirty assembly, first testing, disassembly, cleaning, clean assembly, in air system identification, and iterative steps of testing and commissioning.

3.1 Dirty assembly

The dirty assembly is presented on Figure 14. The purpose of this first assembly was to check that all the parts fit, measure and minimize the cross couplings via a shimming process. Only the position sensors were used during this first period of tests.

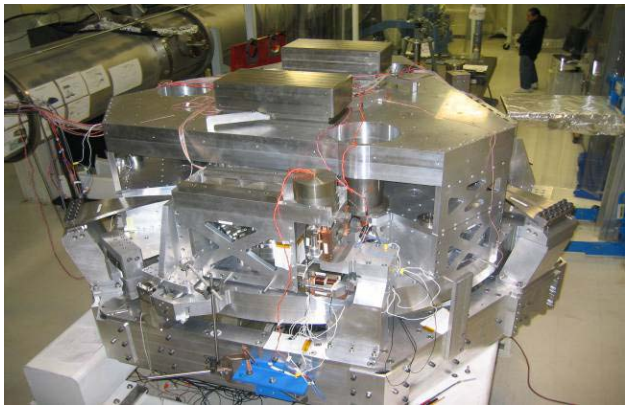

Figure 14

The measurements made showed that the cross couplings were not meeting the requirements. The problem was due to incorrect positioning of the small actuators. The actuator brackets have been redesigned to align the actuators with the zero-moment point of the rods in order to minimize the tilt coupling. Figure 15 shows the actuator in its new position after it had been lowered to be aligned with the zero moment point of the rods.

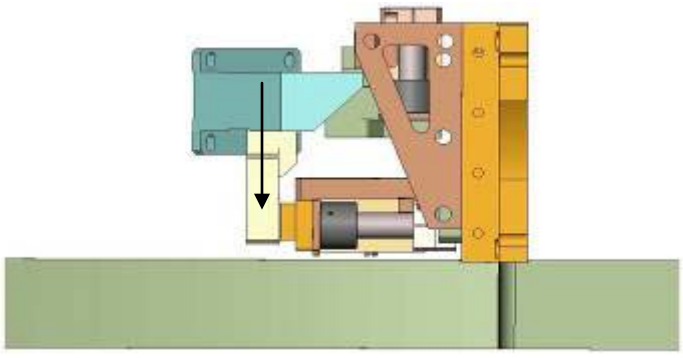

Figure 15

The actuators re-positioning moved the "X to Ry" and "Y to Rx" tilt couplings frequencies from 190mHZ and 170mHz to 60mHz and 90mHz which is a satisfactory result.

The uncertainties and variability on the measurements didn't allow us to compute with enough accuracy shims that would further reduce the cross couplings as suggested by ASI. The shims have

however been redesigned to accommodate a higher load for the next assembly that was going to include the quadruple pendulum.

This first assembly also showed that the blade loading tool needed to be redesigned. Figure 16 shows the current tooling. Its use, as shown in Figure 17, is not completely satisfactory. A third generation will be designed.

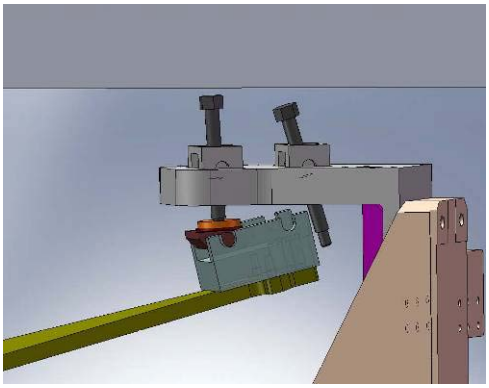

Figure 16

Figure 17

3.2 Components and Subsystems testing

In parallel with the assembly, some of the components have been individually tested. The blades testing showed that the blades stiffness variability was reasonably small.

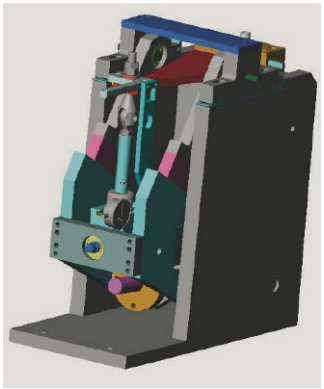

Figure 18: Testing set up

Figure 19: Testing set up

Actuators have also been tested. Results showed that they all had quasi-identical frequency response which is now use in the control filtering. Results are detailed in the document T0900226.

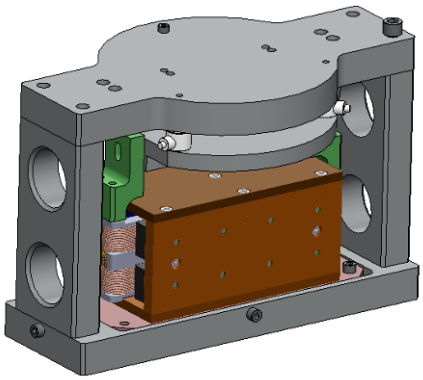

Figure 20: actuator jig.

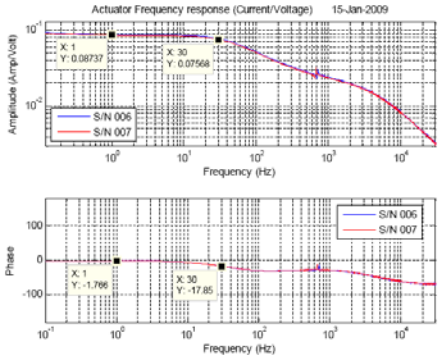

Figure 21: Actuator transfer function

3.3 Cleaning

At the end of the "dirty assembly test period" the BSC-ISI was disassembled. Its parts were sent to cleaning. This cleaning period allowed us to adjust the cleaning process, the facilities, and to solve some cleaning issues as described in this section.

- **Cleaning space requirements and facilities**

The in-house chemical cleaning and oven space limitations were determined. The volume, flow of parts and timeline were estimated for production. Large plate baking capability moved to LIGO: ovens for large parts used by vendor are now at LLO and planned for LHO for in-house use.

- **Cleaning/baking procedures evolved**

The cleaning and baking of positions sensors and SmCo magnets for the movable coil actuators was tested and perfected.

- **Cleaning issues**

Discovery of machining scraps: the machining process left scrap metal in blind holes. We determined what to look for and specify for machining. Figure 22 pictures some of the scraps found in the blind holes.

Figure 22

Insufficient cleaning of large plates: the cleaning process for large plates was insufficient to clean the blind holes. Figure 23 shows how the holes in the large plate had to be cleaned one by one. Figure 24 shows the residual chemicals removed. The chemical cleaning process was insufficient but would be OK if these holes were through holes. These blind holes will be eliminated in the new design.

Figure 23

Figure 24

3.4 Clean assembly

During the clean assembly, careful attention was given to assembly issues. A change design list was compiled that would address these issues. This section describes the main problems identified during the clean assembly.

- **Issues with clean parts**

Galling of screws: many of the stainless steel screws needed to be replaced with silver plated screws.

Tooling, friction in lockers: Looser tolerances had to be used for some parts such as the locks. In the dirty assembly the lock sleeves fit into the housing easily but once cleaned these locks were too sticky to assemble. A couple of coatings to prevent friction were tried but widening the housing worked best.

Figure 25

Figure 26

- **Access to bolts**

It was discovered that some bolt positions did not provide for wrench or hand access. This will be fixed in the final design.

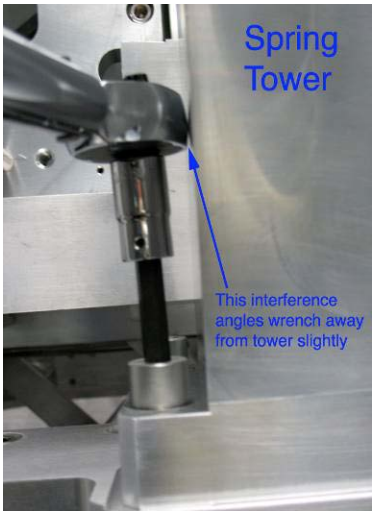

Figure 27

Figure 28

- **Actuators and Surrounding Brackets**

The installation of the actuators was difficult, very long, and required several iterations to adjust the gaps between the coil and the magnet.

The actuators were re-designed:

- to increase gaps around the coil in the actuator to make centering of coil easier

- to change brackets to eliminate over-constraint of the position of the actuator coil.

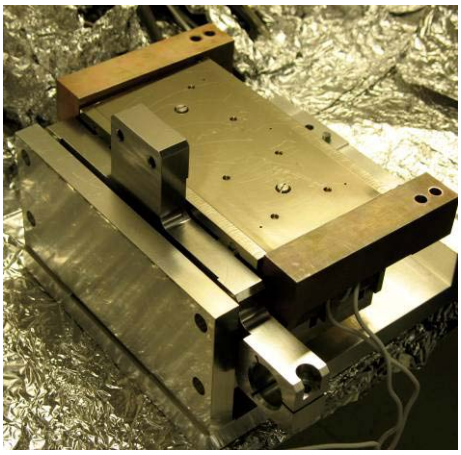

Figure 29

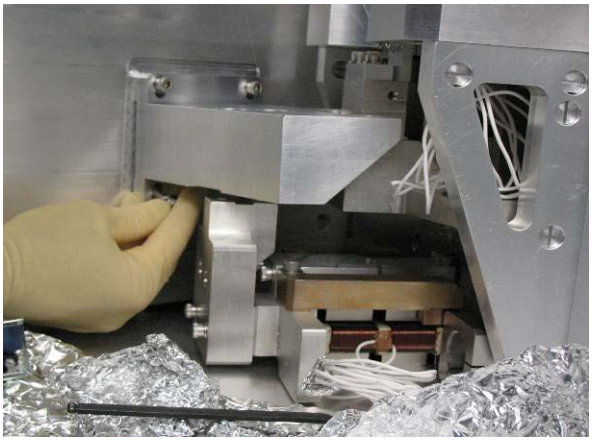

Figure 30

- **Alignment of Flexure Rod and Blade Spring-**

At the end of the assembly, Stage 1 was strongly unbalanced. The height asymmetry from one corner to another corresponding to this unbalance was close to 50mils. We found that one of the shims was not well seating in its cutout as shown in figure 32. It means that the flexure rod can jump out of its seat at the end of the blade spring during the loading.

The current flexure rod is held in the spring by tension once the spring is loaded. The re-design we are currently implementing will allow aligning and then securely attaching the flexure rod to the spring before the spring is loaded.

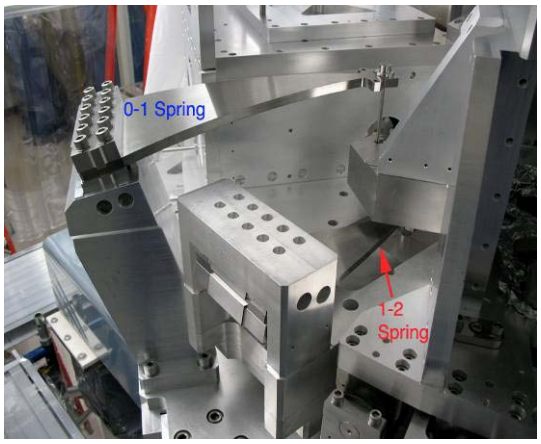

Figure 31

Figure 32

3.5 First commissioning

A series of tests were done on the clean assembly in air. The system identification done in air was focused on the low frequencies (below 30Hz). It showed that the cross couplings were reasonably small, there were no interferences, the transfer functions were quasi-identical in all of the three corners and the suspension resonances were matching with the design. The system was then inserted in the chamber and we started the first commissioning.

The first commissioning was done from June to December 2008. It allowed us to identify three major problems:

- the first deformation resonances were much lower in frequencies than required.

- the modal density at high frequencies was higher than expected.

- the plant was variant in time.

The figures below present an example of transfer functions from the small actuators to the GS13. The deformation modes were as low as 45Hz, while the requirements specify 150Hz. Figure 34 shows the modal density. Most of those modes have to be filtered out in the control process. This results in an unacceptable loss of phase and consequently of performance. It also makes the control design extremely time consuming and limits the control robustness.

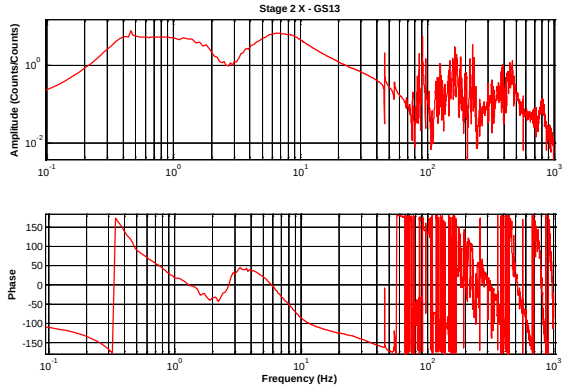

Figure 33

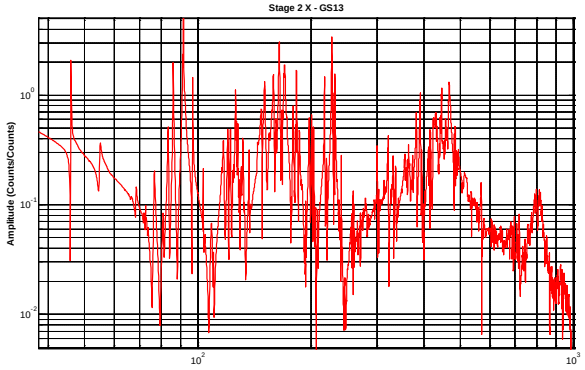

Figure 34

The figure below shows that the plant was not time invariant. The resonances were shifting from one day to another. Some frequencies changes as big as 1.5Hz were observed

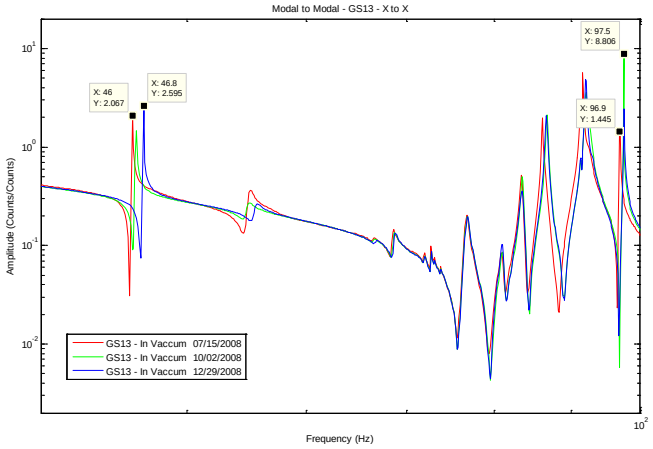

Figure 35

This plant variability was the main limit of the control performance and a source of instabilities. We adjusted the control iteratively according to the plant changes and finally fully controlled the 12 degrees of freedom of the system. An example of performance is presented below. The black curve shows the HEPI motion which is the input disturbance of the BSC-ISI. The blue curve shows the motion of stage 2 when the control is off. The system provides passive isolation as expected above 7Hz. The magenta curve shows the motion of stage 2 with the control on. It provides active isolation from 0.25Hz to 10Hz.

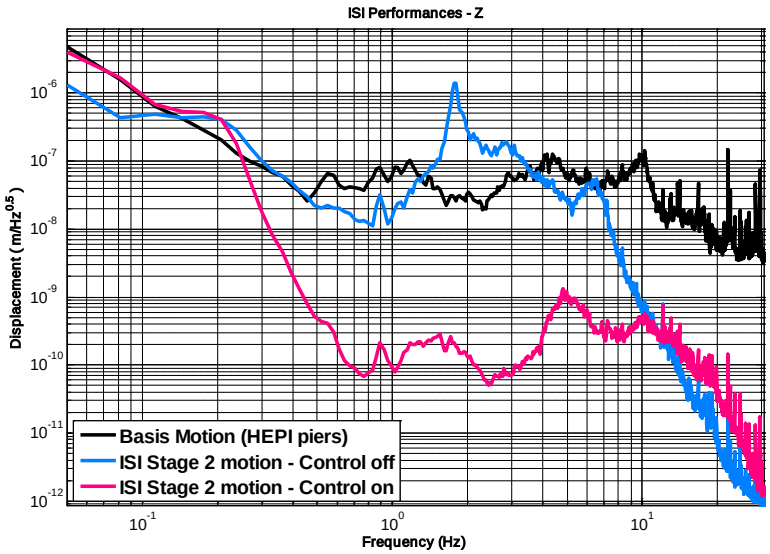

Figure 36

The figure below is an example of global performance as of November 2008. The black curve shows the motion of the ground measured with a STS. The red one shows the motion of stage 2 with the control on. The blue curve shows the requirements. This plot shows the big gap that existed between the performances and the requirements above 4Hz.

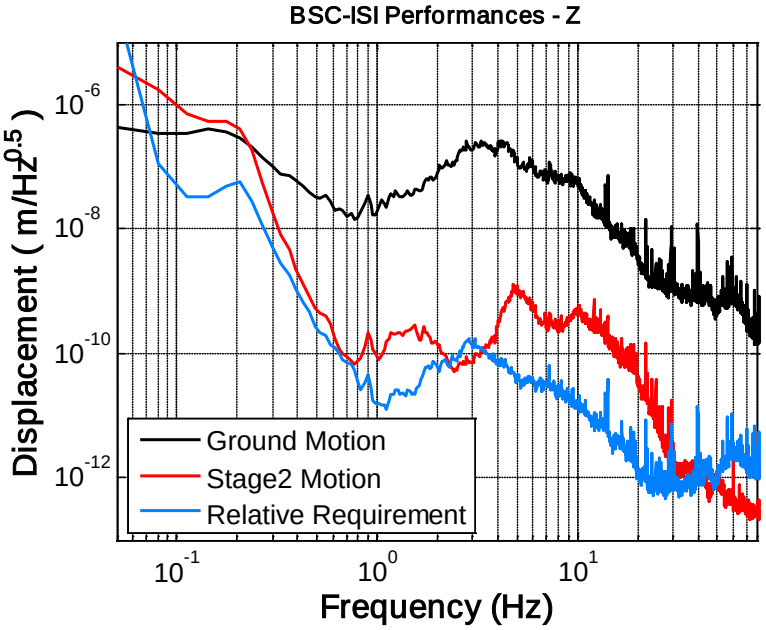

Figure 37

At this stage of the control commissioning we decided we should stop the control development and investigate the sources of resonances and the plant variability. This was necessary in order to make the control more robust and to improve the performance.

3.6 Testing and hardware modifications

In early 2009 the chamber was re-opened and we started to investigate the low frequency deformation modes, the reasons of such a high modal density and more importantly the plant variability. This section summarizes the results of this investigation.

- **Modal testing**

During the first part of the investigation, we worked on identifying the modes causing problems. We used a modal testing approach based on transfer functions from impact hammer to accelerometers. Those measurements are detailed in the document E0900028-v1.

The testing allowed us to correlate some modes in the quad transfer function with some modes in the BSC-ISI transfer function as shown on the plot below. We suggested we should continue the investigation on the use of damping braces between the quadruple pendulum structure and the optical table. However it showed that the quad was neither the source of the high number of resonances nor the cause of the shifting modes. We continued the investigation by studying the other stages.

Figure 38

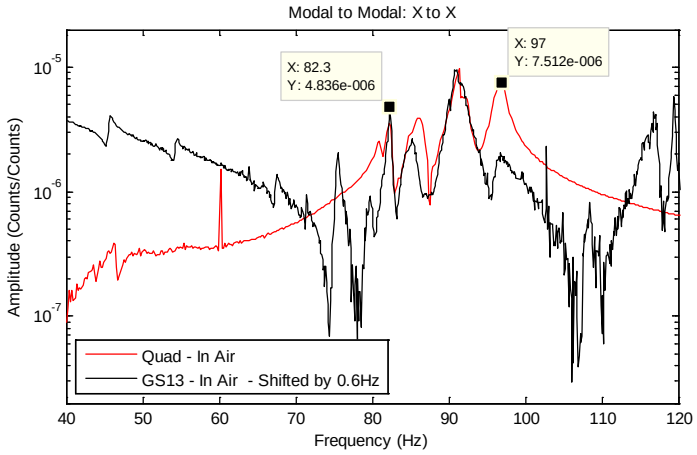

Figure 39

- **Cantilevered seismometers:**

We suspected that some resonances could be induced by the motion of the GS13 pods. Those pods are mounted cantilevered. Some brackets have been machined and installed to lock the free end of the pods. Figure 40 shows a bracket installed on the vertical GS13 pods. These experiments improved the transfer functions for both the horizontal and vertical seismometers.

Figure 41 shows that most of the resonances between 100Hz and 200Hz are directly linked to the cantilever state of the pod. A permanent solution will be implemented in the final design so that the pods will be fully clamped on both sides. This is currently under development as described in section 4.4.

Figure 40

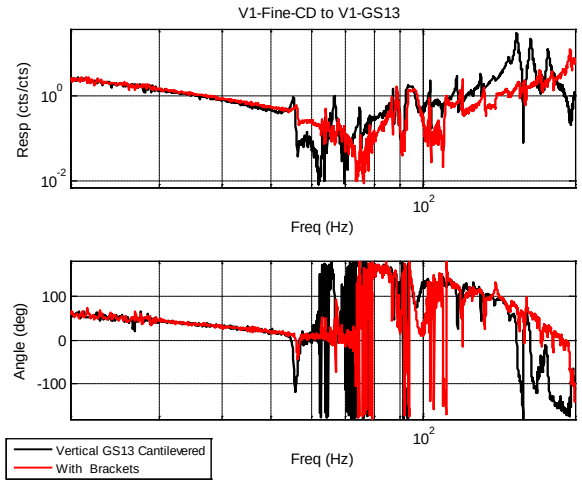

Figure 41

- **Trim masses:**

We found that the trim masses (counter weights) were one of the biggest sources of resonances. Those trim masses are 6in diameter, 10 lbs cylinders of stainless steel. They can be attached on top of each other by a single bolt attachment. They are used for the balancing of the stages. 500 lbs of trim masses are currently in use on stage 1 with only one location available in each corner. An example of a high stack of trim masses in presented in Figure 42.

Brackets and trim masses have been re-machined in order to split these columns and attach them in various locations. Figure 43 shows the improvement on the transfer functions after we had relocated and re-attached the trim masses on stage1.

Significant improvements were also obtained on Stage2 transfer functions by minimizing the height of the stacks. Those trim masses and their attachment to the stages will be redesigned for AdL.

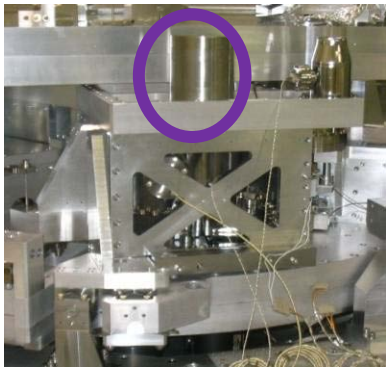

Figure 42

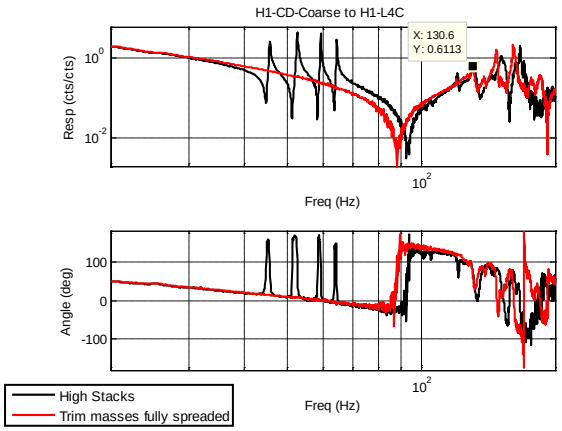

Figure 43

3.7 Second commissioning

The chamber was closed on May 5, 2009 after several months of investigation on the sources of resonances for the combined BSC-ISI-Quad system. The solutions implemented on the hardware and described in the previous section helped to significantly improve the transfer functions and to reduce the number of modes. More importantly, the plant is now time-invariant which was imperative in order to get high control performance. Figure 44 shows measurements made on stage 2 at 3 different dates. The transfer functions are quasi-identical, the only difference noticeable being in the Qs, which is due to the use of different frequency increment for these measurements.

We are now satisfied with the ISI transfer functions. More minor details are now under investigation. For example we are trying to understand why the tilt frequency is so high in the vertical seismometers as shown in figure 45.

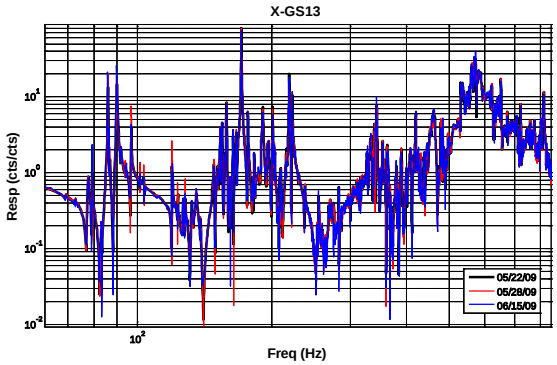

Figure 44

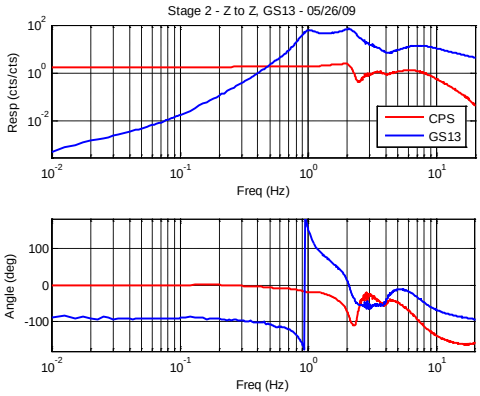

Figure 45

The performances obtained during with second commissioning are presented in section 8.

4 Final Design

The final re-design started on February 2009. The purpose of this re-design is to implement the changes necessary to solve the problems identified during the testing period as described in the previous section. The re-design has been divided in sub-projects: Stage0, Stage1, Stage2, Pods, Actuators and Flexure Rods. The design changes implemented in each of these sub-projects are presented in this section.

4.1 Stage 0

The prototyping phase highlighted several assembly issues related to Stage 0 (most of them are listed in the Design Change List on the SEI Wiki). First, the assembly was long and complicated due to the large number of parts. Secondly, the top surface of stage 0 was not meeting the flatness requirements once it was assembled and loaded. This had consequences on the rest of the assembly since the top surface of stage 0 is the reference plane for the assembly between the stages. As shown in Figure 46, the top surface of Stage 0 supports the blade posts and the tooling for positioning Stage 2 relative to Stage 0. It also supports the actuator posts not shown in this picture.

Figure 46: Advanced LIGO BSC prototype at LASTI

The goal of the Stage 0 redesign was therefore to stiffen the structure and simplify the assembly process. The design constraints were to keep the same footprint for the attachment with other components and minimizing the weight gain. A monolithic approach has been chosen to serve these objectives without an excessive increase in manufacturing price. This option reduces the part counts from 29 to 2, as can be seen by comparing Figure 47 and 48. It also greatly diminishes the number of bolted connections.

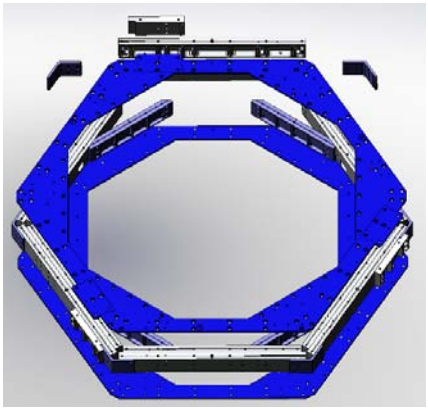

Figure 47
Exploded view of Adv LIGO BSC Stage 0 as built at LASTI

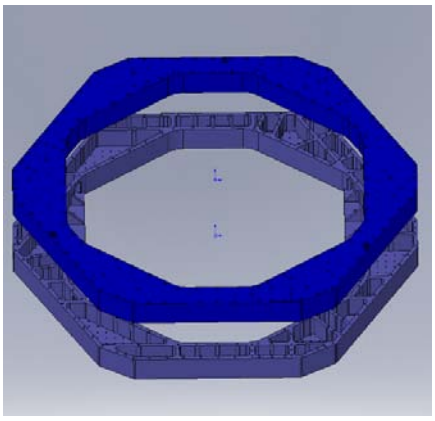

Figure 48
Exploded view of the redesigned Adv LIGO BSC Stage 0.

A preliminary FEA analysis of Stage 0 prototype demonstrated that the load (weight of the other stages applied through the Stage 0-1 springs) was unevenly distributed relative to the support tubes holding Stage 0, resulting in a tilt of Stage 1 (G0900457-Slide 10). A modal analysis was also conducted which showed the weakest parts of the structure (E0900177-v1).

The overall shape of Stage 0 was kept hexagonal and the positions of the blade posts, assembly tooling and lock downs are identical to ASI design. The interior opening of Stage 0 matches the one from the prototype, Stage 0 was made 1.75" wider on all sides and can therefore now accommodate the blade posts without the side excrescences of the prototype.

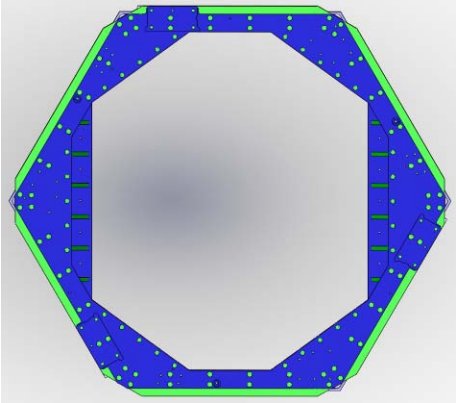

Figure 49
Top view comparison between Stage as built at LASTI (blue) and its redesign (green)

To avoid a large weight gain, deep light-weight pockets were cut out from both parts, while maintaining a 0.8" webbing to allow better resistance to the static deformation and sufficient bolting of the two 550 lb parts. Side walls, bottom and top plates are 1" thick. We reinforced the webbing perpendicular to the support tubes which reduced the displacement of the stage 0-1 springs due to the deformation of stage 0 (FEA-cf G0900457-Slide 10). Supplementary webbing was also added on the interface between Stage 0 and the support tubes.

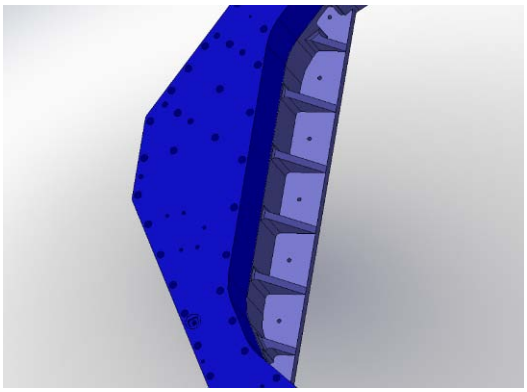

Figure 50: Additional webbing above the support tubes

Six holes have been provided in each part for their manipulation (visible in each corner of Stage 0 in Figure 51). Holes and fixtures were added to attach 3 breadboards on the top plate, as well as 3 vertical L-4Cs and 3 horizontal L-4Cs on the top plate that might added (Figure 51).

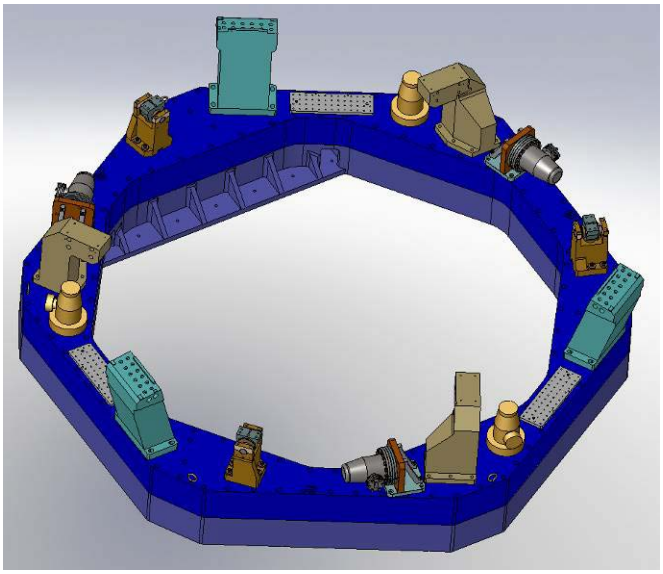

Figure 51 Real Estate on Stage 0- The actuator posts (mustard yellow), lock-downs (orange), and blade posts (cyan) were on the LASTI prototype, whereas the vertical L4-Cs (yellow), the horizontal L4-Cs and the breadboards (grey) were added in the redesign.

A 2" hole pattern was created on its bottom for the attachment of laser beam baffles. The consequences of the baffles resonances on Stage 0 need to be investigated

We will not be using heli-coils for Stage 0 assembly, apart for attaching the posts.

Pins will be used to allow precise positioning of the 2 parts of Stage 0, as well as to position the Stage 0-1 blades posts, actuator posts. The blade post feet will be slightly enlarged to facilitate their attachment to Stage 0.

Stage 0 will be entirely made from AL 6061-T651, instead of the former combination of AL 7075-T651 (not recommended by the vacuum board) and AL 6061-T651.

The most recent mass estimate is 1200 lbs without hardware, which represents an approximate weight gain of 23% relatively to the LASTI prototype. (If taking into account the Stage 0-1 elements - actuators, lock-downs and blade post assemblies-,the approximate weight would be 1780 lbs plus hardware) On the other hand, we expect the mass of the hardware, to decrease from 110 lbs in the prototype to 80 lbs due to the diminution of bolted connections. This results in a total increase of 200 lbs, which the SEI team decided acceptable.

4.2 Stage 1

There were three main objectives in the Stage1 re-design:

- Re-designing the connection and positioning of the parts. The initial assembly was based on the use of cut outs for the positioning of plates. The assemblies made at LASTI showed that this approach didn't allow an accurate positioning of the parts. It has been decided to remove the cut outs and replace them by pins for the positioning.

- Implementing the changes as listed in the design changes list established during the prototyping phases.

- Improving the stiffness where it can easily be made. The system identifications and control commissioning showed that Stage1 was not meeting the stiffness requirements and an improvement of the overhaul stiffness of the stage could be a great help in order to improve the control performance.

- **Parts Positioning**

Figure 52 shows the initial base plates and its cut outs used for the positioning of the parts attached onto it. Figure 53 illustrates the changes implemented on the base plate: the cut outs have been removed and pins are inserted for the positioning of the parts. The assembly procedure based on the use of pins is described in the document LIGO-G0900461-v1, BSC-ISI Stage 1 Internal Review.

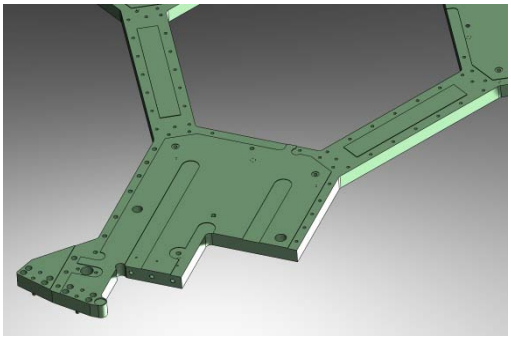

Figure 52

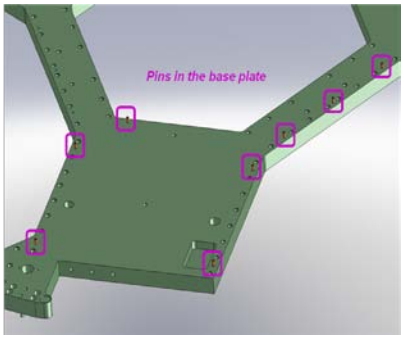

Figure 53

The figure below illustrates the positioning principle: The base plate has pins as shown on *Fig1*, the side plates has slots and holes as shown on *Fig.2* and *3*. The parts are then positioned on the base plate and ready for bolting.

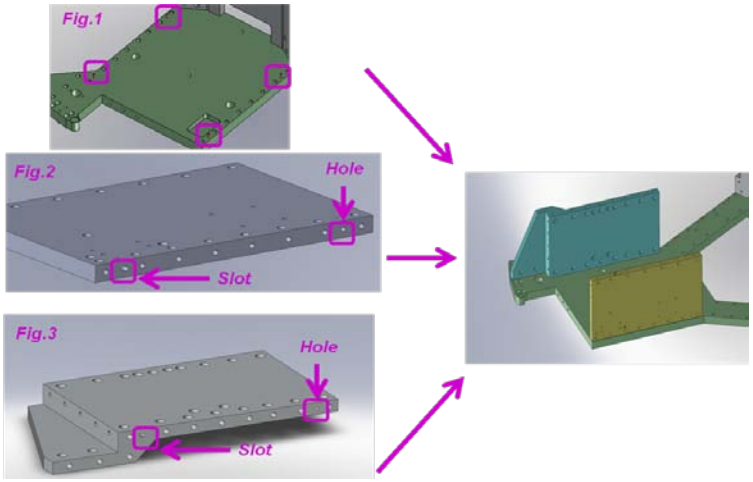

- **Change design list**

Figure 54 illustrates the items of the change design list relative to stage1. They are under implementation:

- item #5: the diameter of the counter bores are increased on the top plate.
- item #6: the position of some barrel nuts is adjusted to make the access to them easier.
- item #18: the horizontal L4Cs have been raised. There is no more risk of interference with Stage 2.
- item #32: some holes on the doors were misaligned. We are repositioning them.
- item #42: the design of the tooling posts used for the initial positioning of the stages will be adjusted as part of the FDR.

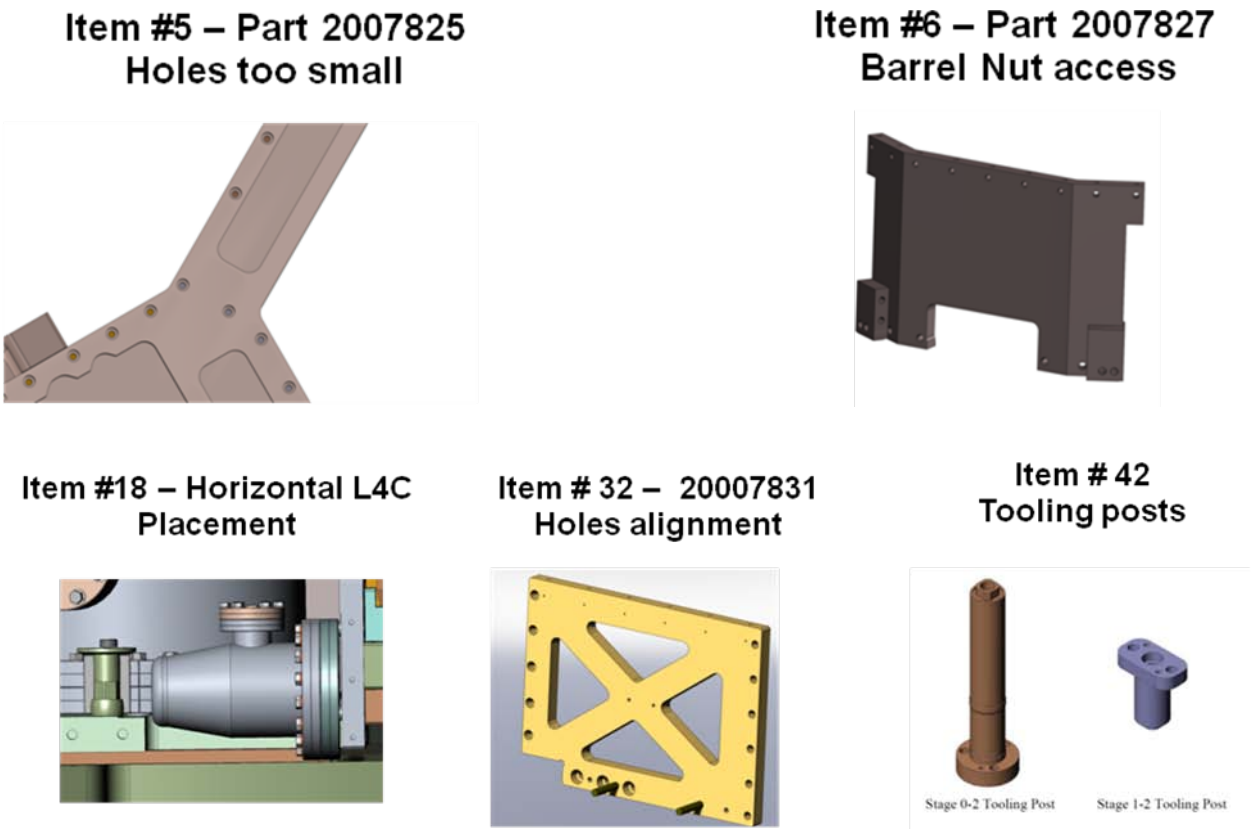

Figure 54

- **Stiffness improvements**

Three structural changes have been implemented as represented on Figure 55.

- The "L4C hole" in the base plate has been filled.
- The connection between the inner walls has been reinforced.
- The close out plate envelope has been extended.

None of those changes affects the position of the major components of the system: actuators, flexure rods and connection between the stages.

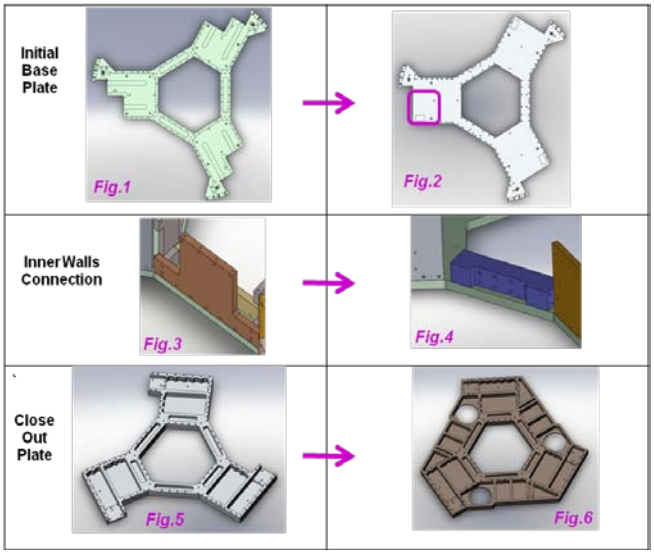

Figure 55

Structural change #1: Hole in the base plate

Figure 56 shows the position of the horizontal L4C in the initial design. One of the initial design requirements was that the seismometers be collocated with the actuators. In order to respect this requirement and to accommodate the L4C, the base plate has a cutout as shown on figure 57. As a result, the part of the wall supporting the L4C and the horizontal actuator was cantilevered. This resulted in a local deformation and twist of the components as illustrated on figure 56 by the magenta arrow.

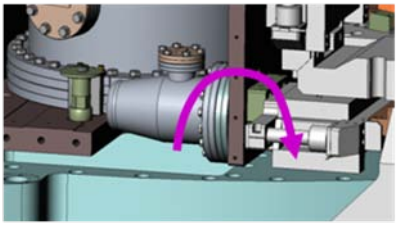

Figure 56

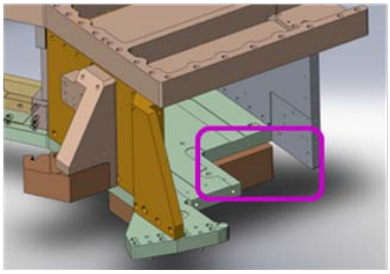

Figure 57

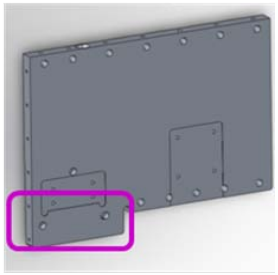

Figure 58

We decided that it would be better to slightly move the sensor up so we can remove this hole in the base plate. The L4C has been raised by 1.5" as shown on figure 61. Only a pocket is then necessary in the base plate in order to accommodate the L4C as shown on figure 59. The wall is now fully tightened to the base plate as shown in figure 60.

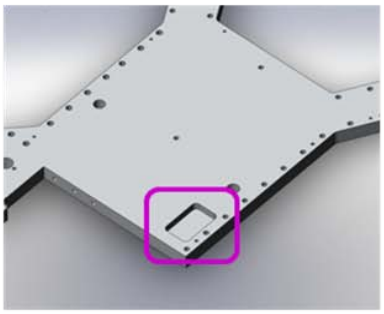

Figure 59

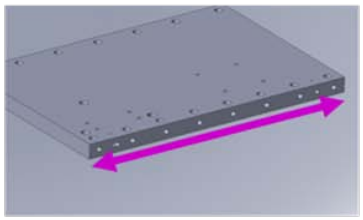

Figure 60

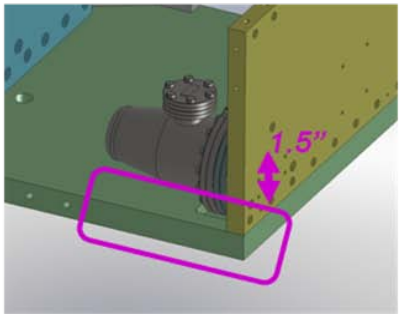

Figure 61

Structural change #2: Connection between corners

A finite element model of stage1 has been done to study its modes of deformation. One of the main modes of deformation is the twisting mode shown on figure 63. This shows that the three corners are rigid but they move relative to each other due to a weak connection between the corners.

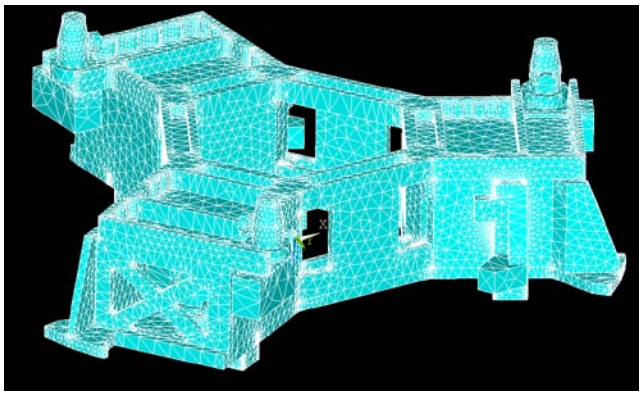

Figure 62

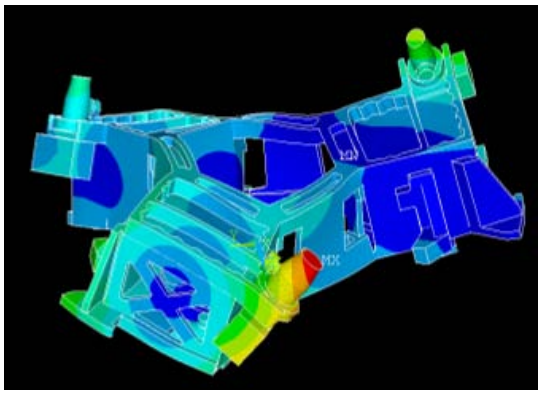

Figure 63

The weak area is presented on figure 64. The new design is presented in figure 65. It is based on the use of the block represented in violet.

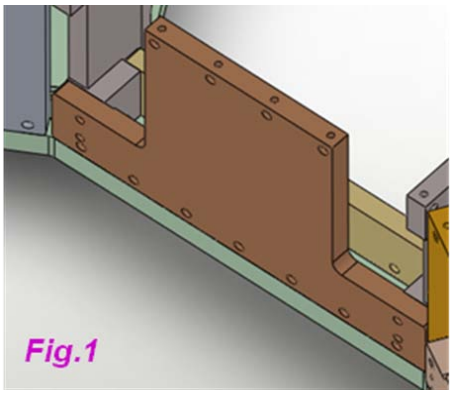

Figure 64

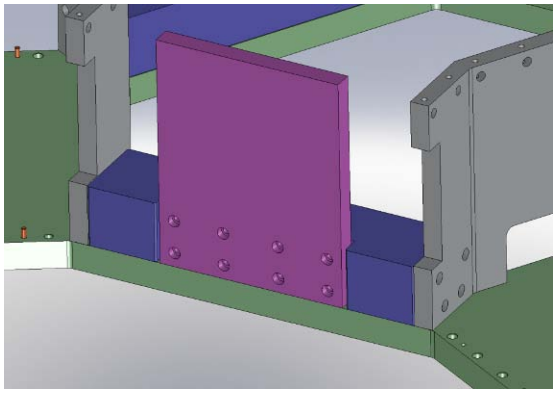

Figure 65

This block shown on figure 66 has been designed to have a good resistance to torsion as shown in figure 67.

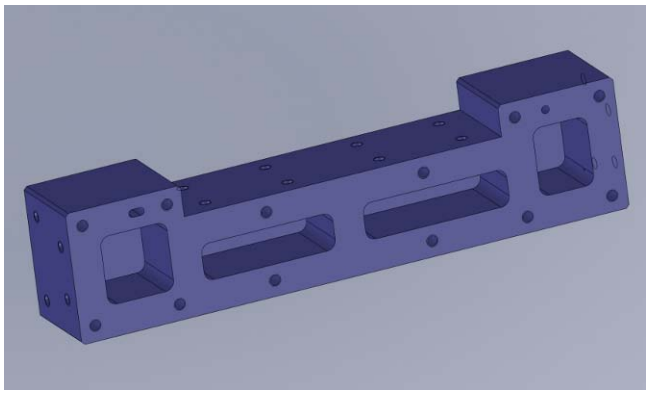

Figure 66

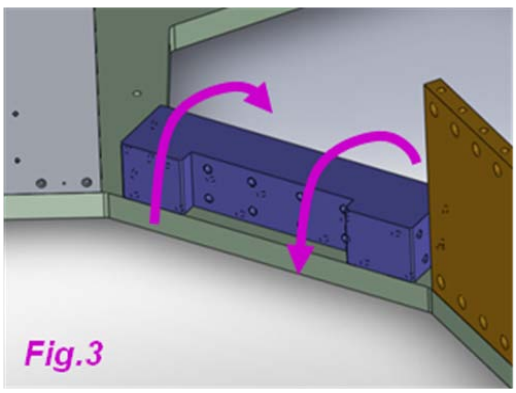

Figure 67

Structural change #3:

Two other sources of resonances were the relative motion of the corners in plane as shown in figure 68 and the local deformation of the vertical L4C-actuator block as shown on figure 69.

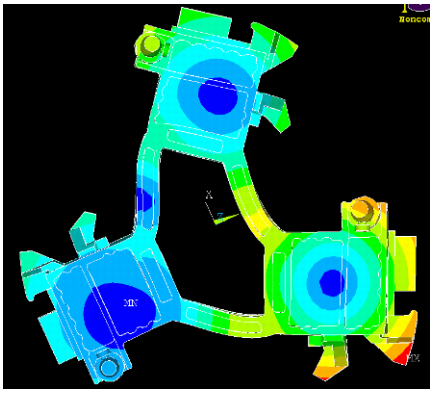

Figure 68

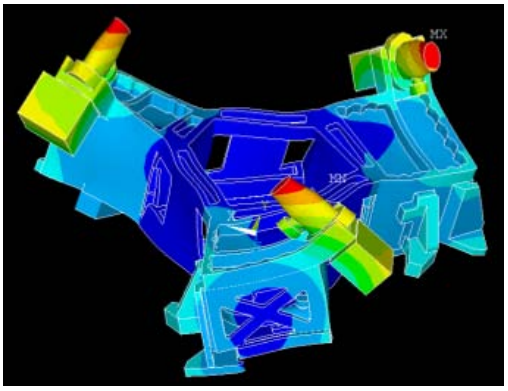

Figure 69

The design of the close out plate has been adjusted in order to reinforce the structure and minimize these deformations. Figure 70 shows the initial design and figure 71 shows the new design. The area between the corners has been filled to provide maximum stiffness. The hole allows the installation of the vertical GS13.

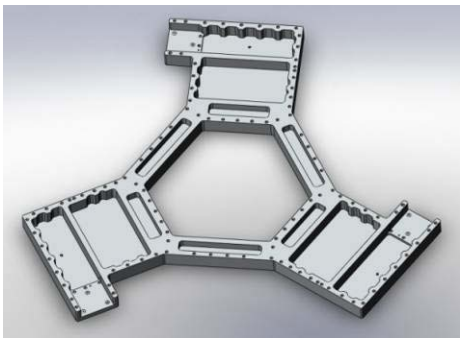

Figure 70

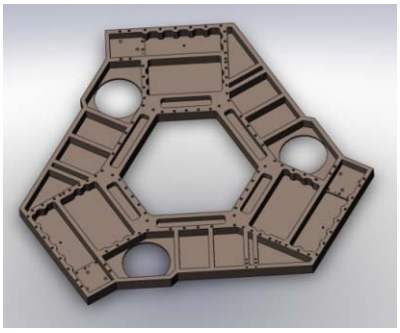

Figure 71

These design changes have been discussed and approved at the internal design review held on 5/29/2009. We are now working on the detailing for the FDR.

4.3 Stage 2

The LASTI prototype Stage-2 is functional, but is in need of simplification and improvement in several areas including: reducing the total number of parts, reducing expensive custom hardware, decreasing overall complexity of assembly, improving modularity of sub assemblies, easing the cleaning of blind holes, including proper venting for unavoidable blind holes, and accurate location of critical components by addition of alignment pins. An additional goal is to increase performance of the structure by increasing the stiffness where ever possible.

The design changes have been presented in the document LIGO-G0900513-v1, Stage 2 Re-Design Status Report, BSC ISI, Advanced LIGO. The main feature of stage 2 re-design are presented below.

Increased structure stiffness, and some parts reduction is achieved through replacing the multi-part walls with single part walls in the center of the structure, as seen in the figure below. Machined part count is also reduced from 15 parts per hex to 12 parts.

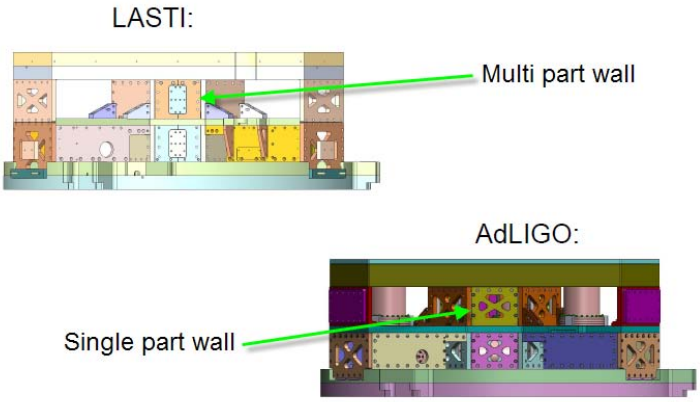

Figure 72

Increased modularity is shown in figure 73 in the "box work" sub assembled that can be built on a granite table and then moved to the top assembly as an independent unit.

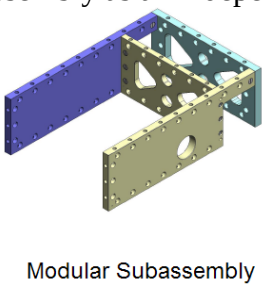

Figure 73

Figure 74 shows how the upper half of the optics table will be simplified by removing multiple datum surfaces in favor of a single full surface datum, and improved structural integrity though the reduced size of large pocks and cuts through the full thickness.

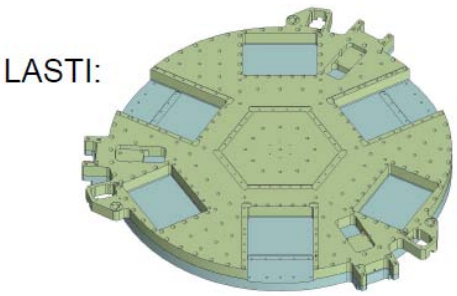

Figure 74

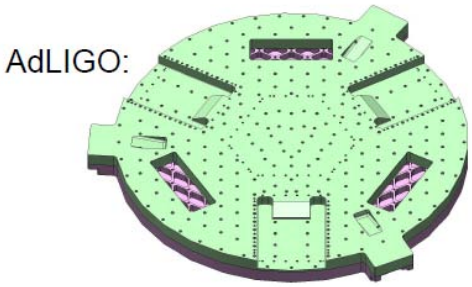

Figure 75

The assembly is described in details in the document LIGO-G0900513-v1. Final assemblies at LASTI and for Advanced LIGO final design are presented below.

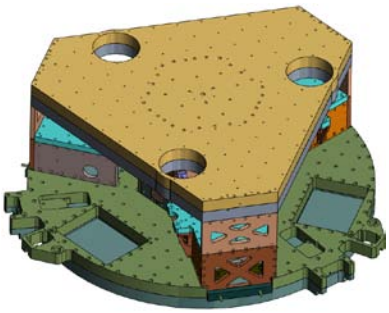

Figure 76: LASTI prototype assembly

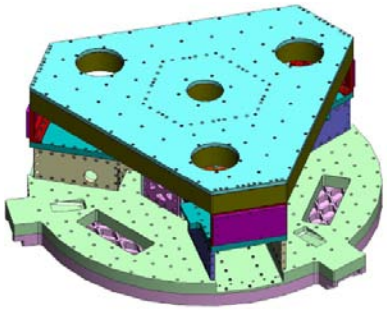

Figure 77: AdL Final design

4.4 Seismometer pods

The BSC ISI is fitted with 3 types of seismometers in individual vacuum pods. There are 6 L4-Cs, 3 of which are located vertically, and 3 horizontally. There are 6 GS-13s, 3 of which are located vertically, and 3 horizontally. There are 3 STS-2s.

The number and general placement of pods will remain the same. The L4-Cs and their pods design were deemed adequate, so there will be no changes to them. The GS-13s were deemed adequate with the flexure change proposed during the HAM ISI FDR and described in LIGO T0900089-v1. There are however a number of performance, assembly and maintenance issues with the pods that needed addressing and modification. The STS-2s are being replaced with Trillium 240 OBSs due to availability issues with the STS-2s, and serviceability issues with the bulky locker motor systems used by them, but not needed by the Trilliums. Thus completely new pods are being designed for the Trilliums.

GS-13 Pod

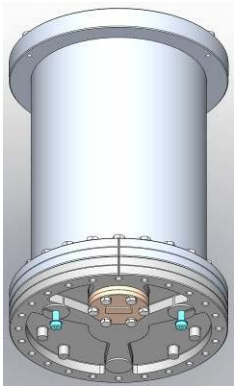

Figure 78

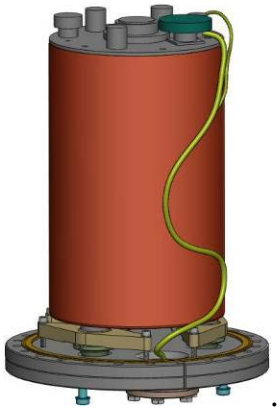

Figure 79

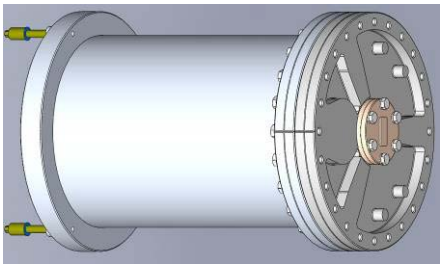

Figure 80

Performance Issues:

The current design of the GS-13 Pod has 2 different configurations, one for vertical orientation (Fig 78& 79) and one for horizontal (Fig 80). Both configurations have performance issues related partly to how the GS-13 is attached to the base flange of the pod, and partly due to the pod being attached at only one end. The horizontal GS-13 has the added issue in that it is attached at the cantilevered end of the pod.

This has resulted in modes being induced by the pod and seismometer interfering with the control of the system. Tests have been performed on both horizontal and vertical pods mounted on the ISI showing that stabilizing the free ends will have a significant impact on improving performance.

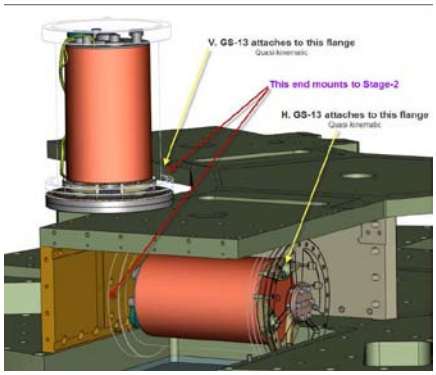

Figure 81

Installations and Maintenance Issues:

Mounting of the GS-13 to the pod is currently done by locating the 3 seismometer feet in a quasi-kinematic setup that is then clamped to the pod base flange (Fig 82). Due to the adjustability of the feet, leveling of the GS-13 is difficult and time consuming. This is particularly true for the horizontal orientation due to the tolerance.

The pod also lacks features to pre-align them when being mounted to stage-2, thus making installation difficult and time consuming. The attachment of the pod to the stage is difficult since access to the fasteners used is obstructed by other components.

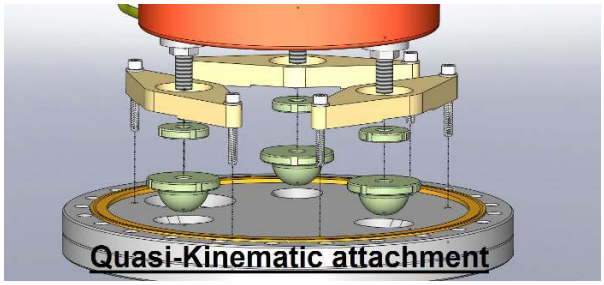

Figure 82

Changes:

The quasi-kinematic attachment and leveling system has been replaced by a single interposed plate between the GS-13 and the pod base flange. Nuts are used to attach the interface plate to the GS-13 and 3 screws are used to attach the interface plate to the base flange. Shim washers were used to provide a 3 point base and leveling capability (Fig 83). This has been successfully tested at LLO.

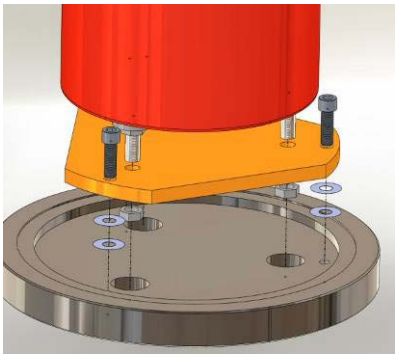

Figure 83

Figure 84

Mounting of the horizontal Pod has been flipped around so that the base flange, to which the GS-13 is attached, is now the same flange that attaches the pod to Stage-2. Also, support for the free end of the pod has been added (Fig 85 & 86). The bosses on the base flange have been moved to the perimeter of the base flange near the clamping points to increase pod attachment stiffness. Additional support for the top of the vertical pod is under design. These improvements will increase performance by increasing the stiffness of the assembly.

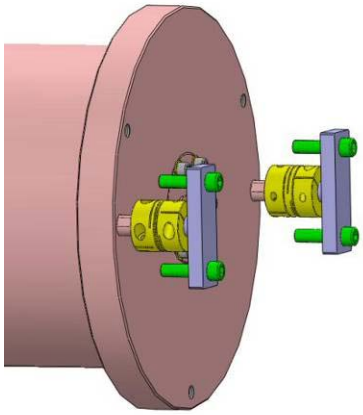

Figure 85

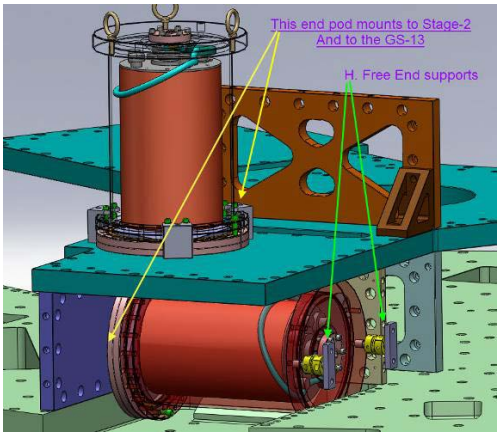

Figure 86

There is now common configuration for the vertical and for the horizontal pod. This was made possible by relocating the feed-thru from the bottom of the pod to the top. This also simplifies the installation, ordering, and reduces cost somewhat. A redesigned pigtail cable will be necessary.

Attachment for the vertical is now done only with clamps (Fig 86). Alignment is provided by locating pins in hole and slot. Due to restricted space, the horizontal pod will be mounted by screws through the stage-2 wall and the exact alignment method will be developed in time for the FDR.

Trillium 240 OBS Pod

Figure 87

Figure 88

Performance:

The all new pod for the Trillium is much like the old STS-2 pod. But, several improvements have been incorporated. The quasi-kinematic attachment and leveling system used internally in the STS-2 has been replaced by a stiff interposer plate between the Trillium and the pod base flange (Fig 89). This automatically levels the Trillium to the base flange. Also the bosses on the base flange have been moved to the perimeter near the clamping points (Fig 90), and the top of the pod is now a full dome . These changes should improve the quality of the transfer functions by increasing the stiffness of the assembly.

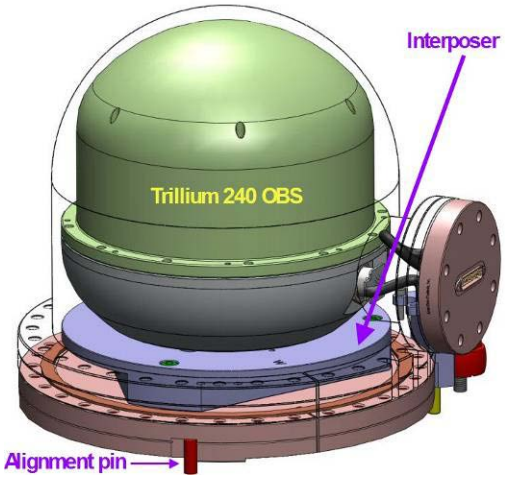

Figure 89

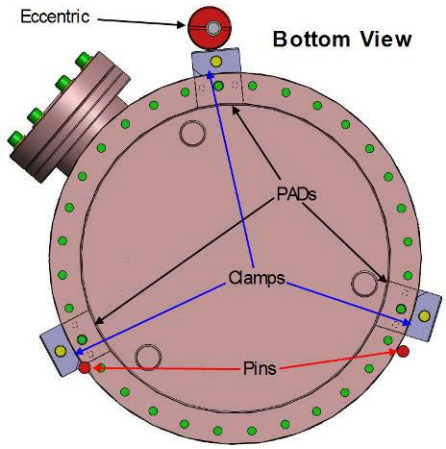

Figure 90

Fabrication, Installation and Maintenance:

The new pod is significantly smaller, and thus lighter, than the STS-2 pod which was 16" max OD and weighed ~115lb. The Trillium pod is 12" max OD, weighs ~73lb with mounting hardware, and still uses standard off the shelf: flanges, tubing and dome. The smaller size and weight should significantly ease installation and removal for maintenance if necessary.

Attachment of the new pod to stage-1 will be done with clamps (Fig 90). Alignment of the pod will be much the same as for the STS-2, where the pod is pushed up against 2 locating pins by an eccentric clamp. Clocking is provided by one of the pins in a recess on the side of the flange (Fig 90). This allows the pod to be installed and removed after ISI assembly is complete.

Vacuum leakage:

An additional benefit of the much smaller pod relative to seismometer volume is the advantage it provides to leak detection of the internal atmosphere out of the pod.

Yet to be done:

- Details of electrical connectors and cabling for both Trillium and GS-13
- Alignment features for GS-13 Horizontal Pod

4.5 Actuators bracketing

The BSC ISI has electro-magnetic actuators used for the active control of the stages. There are 6 large actuators between stage 0 and stage 1; three providing vertical actuation and three providing horizontal one. Six small actuators sit between stage 1 and stage 2, again three vertical and three horizontal. The correct positioning of these actuators helps to reduce cross coupling of the motion of the stages. LIGO document #T0900319 contains historical notes on the actuator re-design.

- **Actuators on the ASI-designed LASTI prototype**

Problems were discovered during the installation of the actuators on the AdLIGO BSC ISI LASTI prototype and a list compiled for re-design. The coil side of the actuator is attached to one stage and the magnet to another. The gap between the coil of the actuator and the magnet must be set and then maintained when the actuator is attached to the stages. This gap ensures that the stages remain independent of one another, attached only at the springs.

Over-constraints in the design of the connection between the actuator and the stage lead to uneven gaps between the magnet and coil, limited range of motion of the actuator before the coil and magnet (and therefore the stages) touched and misalignment of the force direction of the actuators. A summary of the actuator assembly problems on the initial LASTI prototype are noted below.

1. sub-assembly is over constrained with locking bar attached: locking bar and screws that attached actuator sub-assembly to the rest of the ISI fight against each other such that the coil bounces to a different location once the locking bar is removed (this means that gaps between coil and magnet are lost when locking bar is released).

2. gaps in all actuators are difficult to set once actuators are installed—shims on the brackets are not the most elegant way to set these gaps. But the assembly should allow for the gaps to be set with the actuators in place on the assembly rather than ahead of time (e.g. eliminate the need for locking bars).

3. assembly order puzzle—the vertical GS-13 needs to be removed for the fine vertical actuator (and therefore the fine horizontal as well) to be removed

4. for testing purposes the actuators need to be more easily isolated—e.g. should be able to unscrew one end either the installed horizontal or vertical fine actuators so that the whole actuator is only held on a one stage only—this way the other actuator can be tested independently

5. position sensor targets are not easily adjustable—screws are very difficult to get to (fine vertical currently needs a specially cut allen wrench)

6. bracket connecting the horizontal fine actuator may not be a stiff connection (it first attaches to a second bracket, shared with the vertical fine, before connecting to the stage 1 wall)

7. access to the screws to install the fine actuators is very tight—can barely get tools in let alone hands

- **New Actuators and New Brackets**

The actuators, both large (stage 0-1) and small (stage 1-2) have been re-designed and have larger gaps between the coil and magnet. (LIGO document #E0900037-v3 is the statement of work for the large actuators also used on the HAM ISI. This gives the requirements for the new actuator design.) The external dimensions of the actuators changed as well necessitating the design of new brackets to attach the actuators to the stages.

The actuator assembly re-design encompasses both the new size of the actuators and addresses the concerns discovered during the assembly of the LASTI prototype.

An intermediary design (between the original ASI design and the design to be used with the new larger gap actuators to be used in AdLIGO) was done so that we could test the new large actuators at LASTI. The new size of the actuators and the over constraint of the attachment to the stages were addressed. Since major parts on the stages could not be altered due to cost and time this LASTI test could not address all of the concerns listed above. The performance and stiffness of the new actuators and brackets were satisfactory. The assembly still needs improvement and will be accomplished with changes to parts of the stage that could not be changed for this test at LASTI.

Further design changes are recommended for the final design of the AdLIGO BSC ISI actuator assemblies and are discussed below.

- **Design Changes for the horizontal Large**

The original horizontal large actuators had small gaps and over constrained assembly. It is represented on figure 91. The new actuators with the larger gaps have been tested on the LASTI prototype. It attaches to stage 1 wall with intermediary plate and the screws run vertically as shown on figure 92. The position sensor assembly is incorporated in the coil bracket. The target assembly is incorporated in the magnet bracket.

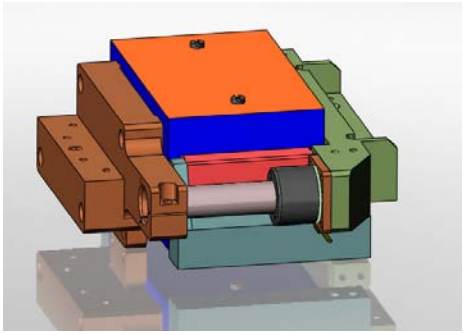

Figure 91

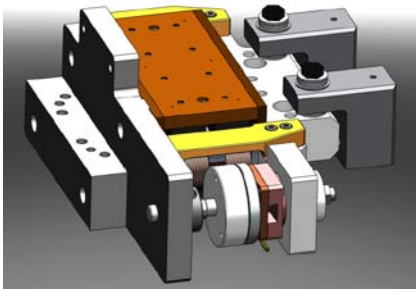

Figure 92

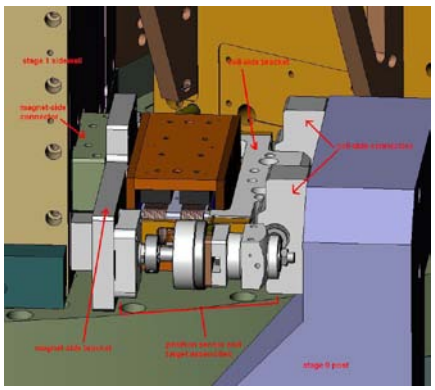

Figure 93: the new horizontal actuator assembly installed on the LASTI prototype.

The final design will include the following features:

- spherical washers between the actuator and the stage ensure that position of the coil vs magnet can be adjust regardless of any misalignment of the stage wall (for example if the stage 1 wall where the magnet attaches leans then the spherical washers allow the coil to match the alignment of the magnet even if the leaning stage 1 wall is not perfectly parallel to the stage 0 post).

- attaches to stage one wall from wall to magnet bracket; screws run horizontally. This will ensure a better connection between the magnet side of the actuator and the stage 1 wall.

- magnet side of actuator is pinned to stage 1 wall to ensure proper height

- target assembly is added to the magnet bracket after actuator installation; position sensor assembly is added later and attached to the coil bracket connectors (L-shaped connectors)

- Changes to Post and Bridge to eliminate cut-outs on post and accommodate newly sized actuators

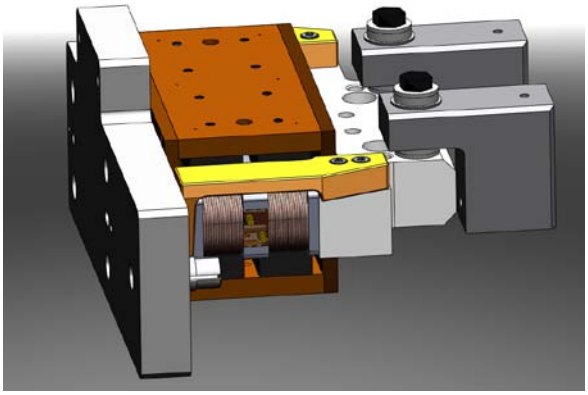

Figure 94

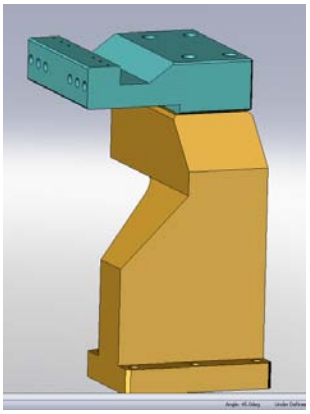

Figure 95

After a design review more changes were recommended and will be implemented in time for the FDR:

-position sensor and target will be far removed from the actuator so that the gaps can be checked later in the assembly.

-the spherical washers will become an option to be added in case of any misalignment of the stage walls. Otherwise thick shim washers will be put in their place.

- **Design Changes for the vertical Large**

The original vertical large actuators had small gaps and over constrained assembly. They are represented on figure 96. The new actuators with the larger gaps have been tested on the LASTI prototype. It's attached to same area of stage 1. Position sensor assembly is incorporated in the coil bracket; target assembly is incorporated in the magnet bracket.

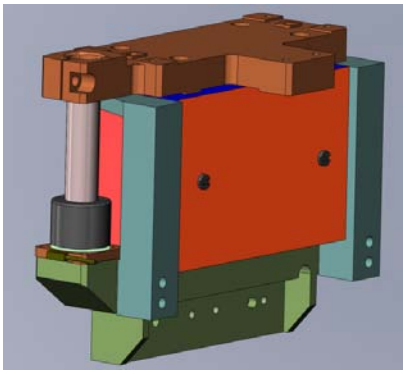

Figure 96

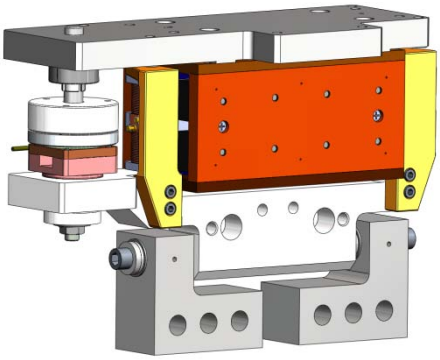

Figure 97

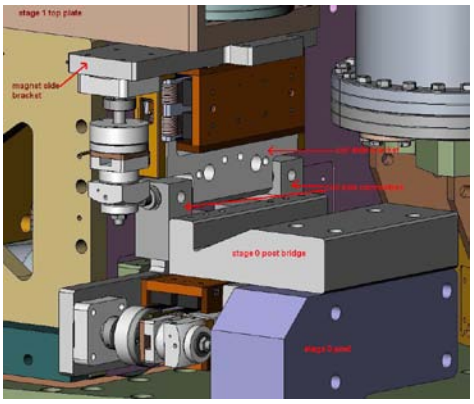

Figure 98: new vertical actuator assembly for LASTI prototype

The final design will include the following features:

-target assembly is added to the magnet bracket after actuator installation; position sensor assembly is added later and attached to the coil bracket connectors (L-shaped connectors)

-taller post and bridge to accommodate location of the new assembly

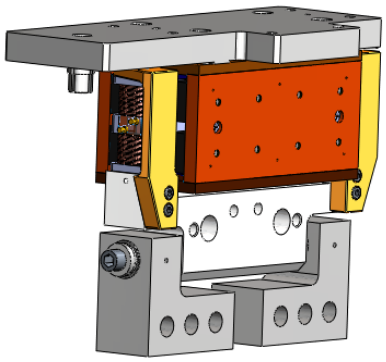

Figure 99

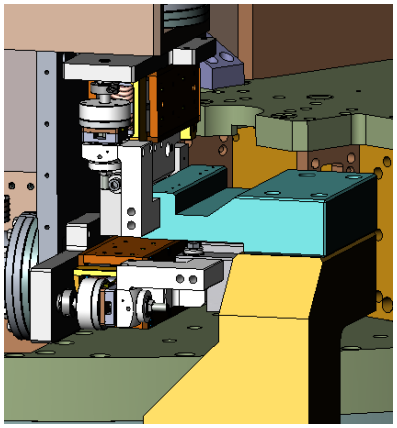

Figure 100

After a design review more changes were recommended and will be implemented in time for the FDR:

- position sensor and target will be far removed from the actuator so that the gaps can be checked later in the assembly.

- the spherical washers will become an option to be added in case of any misalignment of the stage walls. Otherwise thick shim washers will be put in their place.

- **Small Actuator Assemblies:**

Like the large actuators (stage 0-1) the small actuators (stage 1-2) have been redesigned with larger gaps between the coil and magnet. The relative position of the magnet vs coil also needs to be adjustable to accommodate any misalignment of the stage walls or any bulges in the wrapping of the coil wire in the actuator itself.

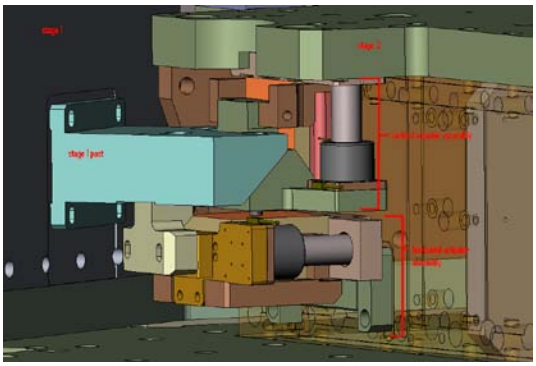

Figure 101: original ASI design of small (stage 1-2) actuator assemblies

Design changes for the small actuator assemblies are yet to be made. The decisions that have been made to incorporate into this new design include:

- A separate position sensor sub-assembly and target assembly will be made to match those on the large actuators. These will be placed in a new position away from the actuators so that the gap between the coil and magnet can be accessed and measured.

- The connection to stage 1 needs to more direct connection to stage 1

- An option for spherical washers between the coil side of the actuator and the stage 1 side wall will be added to accommodate any misalignment of the actuator attachment points on stage 1 and stage 2.

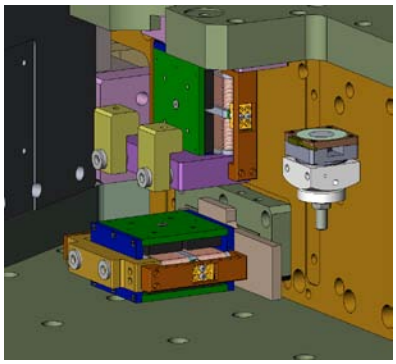

Figure 102: design changes begun on small (stage 1-2) actuator assemblies

- **Yet to be Done:**

-The large actuator assembly re-design needs to be completed to fulfill the decisions made by the SEI design group and listed above.

-The small actuator assembly design is yet to be completed but decisions on the direction of this design is complete as discussed above.

-Tooling has yet to be re-designed for the pre-assembly of the actuator assemblies.

A decision was made during an SEI meeting as to the Dof's needed on this tooling. See elog entry 1394. Tooling: in how many degrees of freedom should this be adjustable. Prevailing thought thus far: Machining tolerances of the bobbin and magnet assembly should be tight meaning that in MOST directions the coil should not need adjustment (in 5 of the 6 dof). The windings however can have some variance in the dimension so we will want adjustment in one dof so that we can make sure these gaps between coil and magnet are even on either side of the coil.

4.6 Blade Tooling

The blade tooling has been redesigned in 2007 and used for the clean assembly. However it didn't work as well as we would have liked. The clearance between the tool and stage 2 is not large enough as shown on figure 103 and the entire loading process is awkward.

Figure 103

Figure 104

Figure shows the last design used. One of the possibilities we are investigating is to bolt the tooling directly on the close out plate. This project is currently under development.

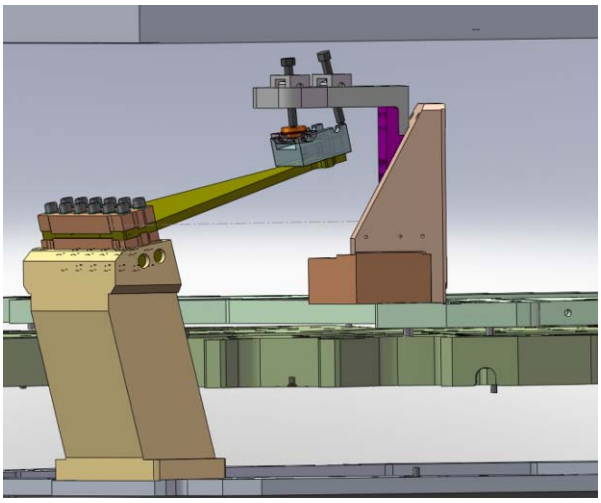

Figure 105

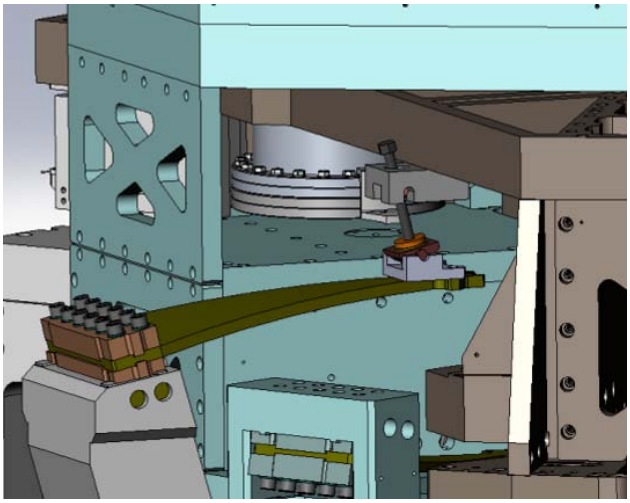

Figure 106

4.7 Rods Attachment

In the initial design, the contact between the blade and the rod was maintained by the contact pressure provided by the axial rod tension. The assembly is described in figure 107. The calculations in section 4 of the ASI Technical memorandum 20009033-A demonstrated that there would be enough friction and an ample margin against slip.

The assemblies done at LASTI however showed that the assembly is difficult, especially for the positioning of the rod on the blade. Some of the assembly issues encountered are described in section 3.4 of this document and illustrated on figure 32.

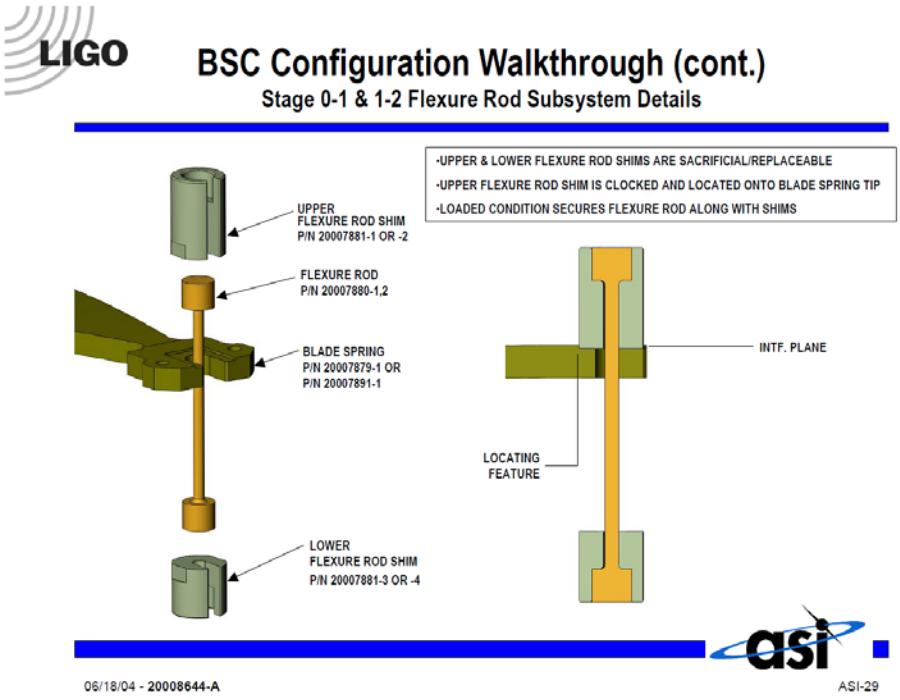

Figure 107

To solve this problem it has been decided that the rod will positioned and bolted to blade. This approach was used by HPD in the HAM Design and worked successfully. The assembly designed by HPD is presented on the figure below:

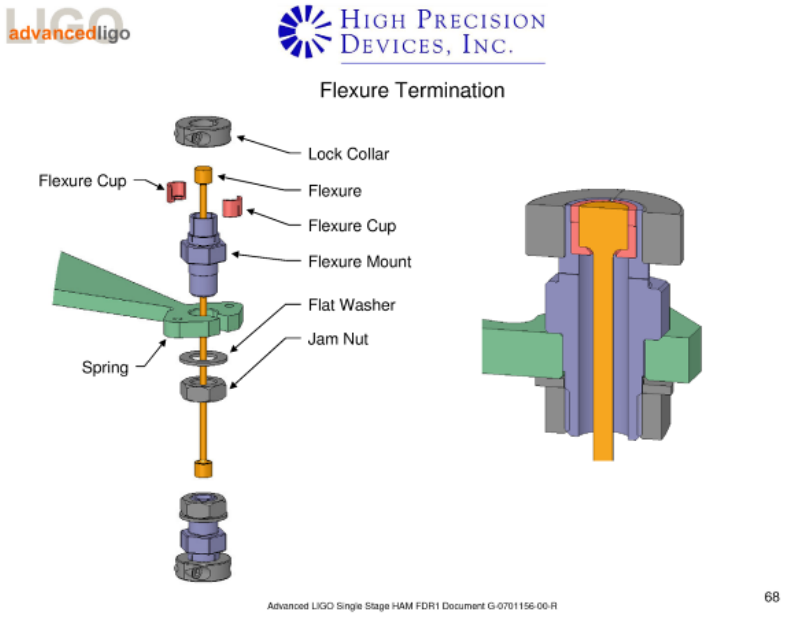

Figure 108

The preliminary design was presented in the document G0900292-v2, BSC ISI Flexure Attachment Kick-Off Meeting. This project is currently under development.

5 Sensors and actuators

The system has sufficient sensors to determine the inertial motion of stage 1 and stage 2 in each DOF, the relative motion between stage 0-1 and the relative motion between stage 1-2 in each DOFs. We also suggest that stage 0 should have inertial sensing in 6 DOFs to enable additional feedforward performance.

On stage 2, the stage closest to the optic, we use the Geotech GS-13 for the inertial sensing and ADE capacitive sensors as the relative displacement sensors between stage 2 and stage 1. The GS-13 is the best 10 Hz inertial sensor commercially available. There are 3 vertical and 3 horizontal GS-13s and 3 vertical and 3 horizontal displacement sensors for stage 2.

On stage 1, where more of the low frequency control is done, we use the Nanometrics Trillium 240 (T240) as the low-frequency inertial sensors and the (relatively) small Sercel L-4C as the high frequency inertial sensors. The T240 is a 3-axis sensor, and so we use 3. There are 3 'extra' channels, all pointed horizontally and radially, which can be used as 2 horizontal and 1 overdetermined DOF sensors, with some coupling to the feedback sensors. There are 6 L-4Cs, 3 horizontal and 3 vertical. For the stage 0-1 relative displacement sensors we again use ADE capacitive sensors. There are 3 vertical and 3 horizontal displacement sensors.

All the sensors on a given stage are combined into virtual sensors with a common coordinate system with an origin at the center of the lower zero moment plane of the stage. Having a common coordinate system minimizes strange coupling behaviors at the blend frequencies where one switches the control from one sensor set to another. Precision of 1 millimeter has been shown to give excellent performance (based on the sloppy holes in the GS-13 mounts on the Tech Demo). Aligning the coordinate system with gravity is critical to address tilt-horizontal coupling. Aligning the coordinate system with the LZMP is convenient, but isn't likely to have performance benefits over any other choice of vertical zero locations. Aligning the horizontal axes with the global X-Y axes allows simple interfaces to the other subsystems.

On stage 0, we plan to put another set of 6 L-4Cs to gain additional 10 Hz sensing for feedforward control to stage 1, similar to the feedforward system being added to the HAM-ISI platforms for the signal recycling mirror and telescope, and with the same 10 Hz target in mind. See 'Discussion of stage 0-1 Feedforward on the Tech Demo' LIGO-T0900135-v1.

Thus, there are 3 types of inertial sensors in use: the L-4C, the GS-13, and the T240. There is only one type of displacement sensor in use, the ADE capacitive displacement sensors, which is setup with 2 different ranges.

5.1 L-4C Inertial Sensors.

The L-4C is a passive geophone with a 1 Hz natural frequency. We equip it with a local preamplifier and place the sensor and preamplifier into a vacuum pod. The L-4Cs have been in use on the Single layer active platform, the 'Rapid Prototype' the ETF Technology Demonstrator, at LASTI, and on HEPI. A discussion of the noise measured from a set of witness L-4Cs on the table of the Tech Demo is described at http://ligo.phys.lsu.edu:8080/SEI/679.

The noise performance is shown below in figure 109.

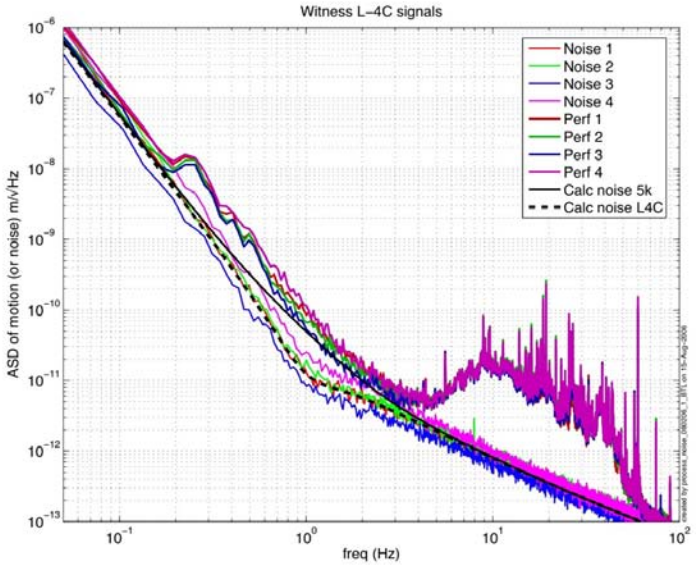

Figure 109: L-4C Noise performance measured with witness L-4Cs on the second stage of the Tech Demo.

5.2 GS-13 Inertial Sensors

The GS13 seismometer is a moving coil seismometer with a 1 Hz natural frequency. It is similar to the L-4C but is larger and has better noise performance. The stock GS-13 can be set to operate either horizontally or vertically. We replace the internal electronics board with one of our own design [D050358-01], which makes this device the lowest noise 10 Hz commercial seismometer available today. A plot of the measured noise performance seen by this instrument is shown in figure 110. The instrument is not vacuum compatible, and so a vacuum 'pod' has been designed to contain the instrument. Twelve of these instruments were successfully modified, placed in pods, and installed in the Observatories on the HAM6-ISI platforms. The instrument modifications, testing, and pod assembly for the HAM6-ISI are described in the 'GS-13 Seismometer Assembly Procedure' [E080086]. A checklist for the assembly of each instrument has also been created. These need to be updated to reflect sensor improvements described below.

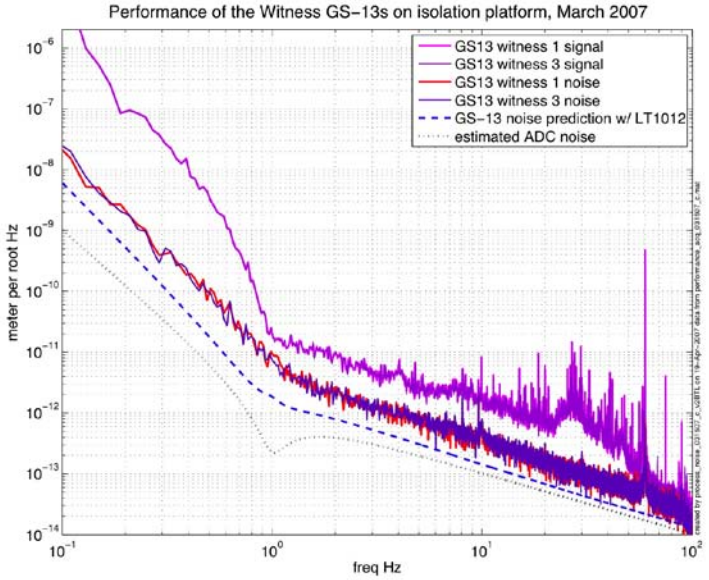

Figure 110: Noise performance of the GS-13s. This measured noise will allow us to reach the BSC requirements.

GS-13 Issues: The podding of the GS-13s for used in the HAM6-ISI platforms was a difficult process. The locking and unlocking of the devices was not as smooth as it should have been. The new units will have custom flexures which can withstand 20 g loads, and so the locking motors are not needed and so will not be installed in all the new units. The flexures and testing are described in LIGO-T0900089, 'GS-13 Seismometer Flexure Report'.

We noticed that some of the units for HAM6-ISI were not well built when we received them from the manufacturer, which caused the proof masses to bind slightly against the locking ring, and made it difficult to unlock the unit. We have discussed this with the manufacturer. We have commissioned a special production run of units for Advanced LIGO to avoid as many of these problems as we have been able to identify (e.g. the calibration coil has been removed, all remaining set screws are secured with threadlocker.) These modifications are discussed in detail in LIGO-E0900027-v1, 'LIGO Project Modifications to the GS-13' and LIGO-C0900025, 'LIGO Review of "Compliance to LIGO Modifications on GS-13"'. In addition, all units will be tested according to our specifications at the manufacturer before shipping and then again at LLO after the new flexures are installed.

5.3 Nanometrics Trillium 240

The Nanometrics Trillium 240 is intended to replace the Streckeisen STS-2 which was originally specified to be the seismometer for low frequencies (below about 3 Hz). The T240 and the STS-2 have similar size, weight, cost and performance. The T240 has several advantages over the STS-2. First, it can be purchased. Requests for STS-2 were met with 18 month delivery schedules and no commitment on whether we would receive the STS-2 or a new STS-3 (about which we know very little). Second, it has no locking motors. The T240 can be shipped (in special containers) without locking motors. Since the retrofit locking motors add size and complexity to the STS-2, and are not very reliable, so eliminating those motors will make the overall system smaller and more reliable. By reducing the size, we have been able to base the new T240 pod on a 12" CF flange instead of the 16.5" flange required for the STS-2. Not only is the new pod smaller (which is an advantage in the crowded BSC system), it has also dropped from 115 to 70 lbs (see section 4.4 about sensor pods). We have recently mounted a T240 (in a pressure vessel) on the optical table of the Tech Demo, and compared the signals with a pair of STS-2s, see T0900318, 'Noise testing of the Nanometrics Trillium 240 on the Tech Demo' (in progress). We do not see significant differences between the noise estimates for the STS-2 and the T240. In this noisy environment, none of the 3 instruments are quite reaching their expected noise performance. It is not clear what the excess noise mechanism is. However, this measured noise estimate is less than the noise used in the performance models, and so, although we expect the real performance is a bit better than we are seeing, the performance we can demonstrate will meet our needs.

Figure 111: Testing sensors at the ETF

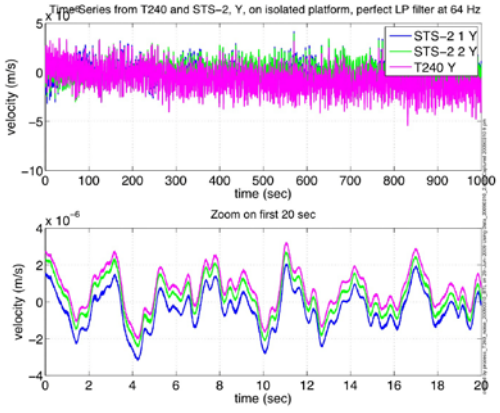

Figure 112: Time history of 3 Sensors

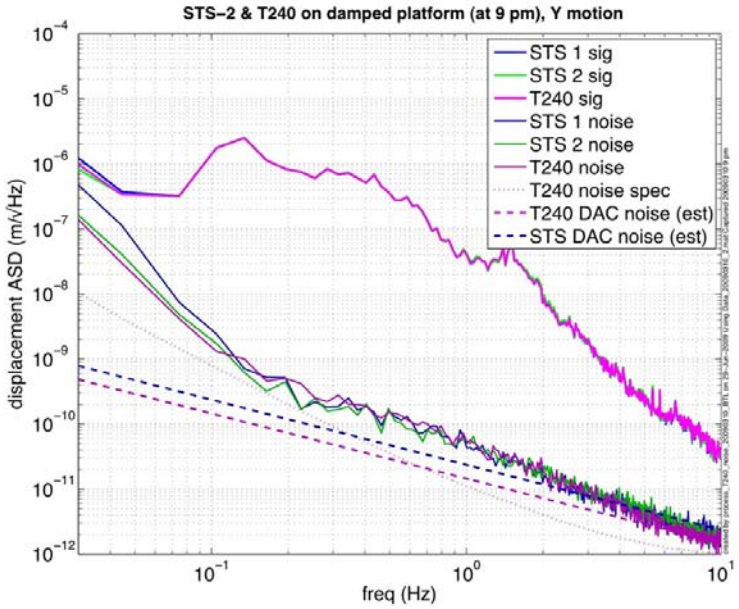

Figure 113: Noise estimates of the T240 mounted on the ETF Tech Demo, and compared with 2 STS-2s and the 6 feedback GS-13s on the stage. The actual motion is about 3 orders of magnitude larger than the noise estimate generated with Wensheng Hua's coherent subtraction technique. We have measured the noise of the STS-2 at 1 Hz to be slightly better than this at 1 Hz when all the isolation loops are running, and so it is not clear why the noise estimates here are not quite as good as we would like. This may result from small nonlinearites in the sensors or readout chains, or may be a result of the mathematical technique not working as expected in the presence of such large signals.

Capacitive Sensors: The capacitive displacement sensors are sold by ADE. They include a UHV compatible head, designed for LIGO, and a readout board. Discussions of the electronics are below in the 'electronics' section below. The sensor range for the stage 0-1 sensors is +/- 1 mm, and the noise floor is around 6e-10 m/rtHz. The sensor range for the stage 1-2 sensors is only +/- 0.25 mm, and the noise is expected to be about a factor of 4 lower (ie 1.5 e-10 m/rtHz) than the stage 0-1 sensors. All the hardware for both stages is identical (same heads, cables, readout electronics, racks, etc). The only difference is the calibration/ sensitivity settings and the matching capacitors in the readouts. The heads are cleaned and baked at low temperature. The heads require a special strain relief for the cable. The heads are provided with special protective stops; calibrated shim washers are used in the installation, so that the heads of the four bolts which attach the sensor head to its mount protrude slightly above the head and contact the target before the head does.

Actuators: LIGO had custom actuators designed and fabricated for the ISI platforms. The design and fabrication is done by a commercial design firm, PSI. The actuators are humbuck wound, square coil actuators which maximize the drive linearity and minimize generation of external magnetic fields. A set of the stage 0-1 actuators have been built and installed for the HAM6-ISI system. The stage 1-2 actuators are of a similar design, but are a bit smaller. A prototype run of these actuators has been delivered to MIT. Since these actuators have potted coils, special cleaning procedures have been developed [E080497] to clean some parts of the actuators before they are fully assembled. The final actuators are cleaned and baked.
Actuator issues: Some minor redesigns of the actuators are being pursued to improve the wire connections. Currently, the stranded drive wires are attached to the actuators at a PEEK terminal block on the actuator. This will probably be modified by adding a crimp pin to the wire, and replacing the slotted bolt on the terminal block with a hex-head bolt. In addition, the kapton-based potting

compound used for the HAM6 installations has been discontinued by the manufacturer and replaced with an upgraded material (PI-2525 resin). The new material is currently being investigated by the LIGO Lab. Tests indicate that it is still UHV compatible [T080148], and still difficult to apply correctly, but it more readily available and ships in more convenient quantities than its predecessor. Also, there are currently unit tests for the GS-13s and the displacement sensors, but we do not have any unit tests for the actuators. It would be useful to have a fixture to hold the actuator with a force gauge, and supply the actuator with calibrated current. This could be used to check the continuity, polarity and force constant of the actuators.

6 Electronics

- **Electronics System**

The entire system is made up of a set of electronics chassis described below, some timing chassis, the "Blue Box" and computer system. The system schematic that shows the interconnection of all of the electronics chassis is found here: BSC_ISI.pdf [LIGO-D0901301-v1].

- **ISI Interface Chassis**

This chassis gathers all of the signals from the GS-13 seismometers, the L4C Geophones and the Capacitive Position Sensors and interfaces them with the computer via an Anti-Alias filter chassis. The chassis contains three main boards, the GS-13 Interface Board: D070115 Rev.B1, the L4C Interface Board, D070126 and the Capacitive Position Sensor Interface Board: D070132. This design is installed in the LASTI ISI system, but some modification is needed for use in Advanced LIGO. All three boards will have their own power switch, so each can be cycled independently. The GS-13 board and the L4C board will, most likely, become the same design because we no longer use the GS-13 lockers, and we have never used the L4C calibration coils. These two features were the main differences in the design thus far. Some of the electronics will be reworked to use better, and more readily available parts. For example, the AD620 chips will be replaced with a lower-noise, and much more readily available LT1125 configuration, and the THS4131 output stage will be replaced with an AD8672 chip. The Capacitive position sensor board will have to be re-done to interface with the new ADE chassis, but the board is really simple, and this should be a relatively easy rework.

- **ISI Coil Driver**

This high-current driver receives signals from the computer via an Anti-Image filter chassis. It provides these high current signals to the ISI actuators. The current Coil Driver Schematics are here: D060454 Rev.D2. The design works well, but some minor internal changes are being done to make the chassis easier to put into production

- **Binary I/O Chassis**

This chassis is essentially a patch-panel that takes one connector that goes to the Binary I/O card, and distributes the signals to the right places. Binary Out signals go to the ISI Interface chassis to control gain and filter settings, and Binary In signals come from fault monitors in the Coil Driver chassis. It is a simple board, but it will have to be redesigned to interface with the newer style of Binary In and Binary Out boards that we will be getting.

- **Anti-Alias Chassis**

This chassis is a low-pass filter for all incoming signals, the cutoff frequency of which is set so that signal frequencies higher than the Nyquist frequency (determined as half the sample frequency) are greatly attenuated so that they don't alias down into the passband. The filters themselves will remain the same as they have been for a while now, the only difference in the BSC ISI version will be its arrangement of frontpanel connectors. All of the boards have 32 channels of available filtration, which correspond to the 32-channel Analog to Digital Converters to which they connect. For the Rev. 12 chassis, these will be split up into 3 25-pin connectors with varying number of signals to each, and one 9-pin connector with two spare channels on it. The 25-pin connectors of one chassis go to one Coil Driver, one ISI Interface chassis, and one Trillium T240 Interface chassis, and distribute the signals to the ADC. The schematic for the filters is here: D070081-01.

- **Trillium T240 Interface Chassis**

This chassis needs to be designed, but it should resemble the STS-2 Interface chassis in use in the HEPI system. It will interface with the Trillium T24 tri-axial seismometer, and send its signals to the computer via an Anti-Alias filter, and an ADC board. It will also receive binary output signals that switch some of the seismometer's functionality.

- **Manufacture and Production**

All chassis will be manufactured at a turn-key external company. They will order the parts, stuff the boards, assemble the chassis, and deliver the whole thing ready for testing, and then delivery to the sites. We are currently examining several of these companies for the manufacture of HEPI electronics, and will select one at the end of a bidding cycle.

- **Setup and Testing of the Electronics**

In testing the system, two boxes and several small boards have been made to help with the task. The first box is the STS-2/GS-13 Tester box. This box is used when a particular seismometer is in an unknown state of health. By plugging this box into a STS-2 or GS-13 pod, one can assess whether the seismometer is working or not. This is helpful during construction, as it means that we can test the expensive seismometer without hooking it up to an untested control system. The GS-13 Controller schematic is here:

GS13_L4C_Controller.pdf. This box gets connected in the place of an in-vacuum seismometer, and allows us to test all of the wiring, and computer system without endangering an expensive seismometer. The Emulator has power supply LEDs that allow you to see, at a glance, if the incoming power is correct before tuning on the Emulator. Once it is on, it outputs a fake seismometer signal that can be detected on the control room screen. There are also LEDs and frontpanel BNC connectors to allow you to check the rest of the computer system functionality. The Emulator schematic is here: GS13_L4C_Emulator.pdf. There are also several boards that help in testing. One is a switch board that emulates the functionality of the binary I/O modules, so gains and whitening can be set right at the rack, and several inline breakout boards that go inline with the cables, and allow you to clip onto any wire inside, and check the health of the signal there. Along with the hardware, we will have good documentation system that provides a system test procedure, and a set of "quick start guides" that let people who might be receiving, or using the electronics have a quick overview of its functionality and "care and feeding". A sample system test procedure from the HAM ISI system can be found here: HAM_ISI_test, and some examples of Quick-Start guides are in these places: GS-3_L4C_Emulator_Quick_start, GS-13_L4C_Controller_Quick_start.pdf, and STS-2_Quick_Guide.pdf.

7 Cleaning, Leak check, Assembly, Storage, and Installation.

7.1 Cleaning

BSC ISI parts will be cleaned to LIGO specifications according to LIGO-E960022. Cleaning and baking of parts except the large plates will take place at LHO, LLO and CIT.

The large plates will be chemically cleaned by an outside vendor and air baked at LHO and LLO. Special procedures, not in the current release version of E960022, used for the actuators and the capacitive position sensors will be identical to those that were used for the Enhanced LIGO HAM ISI. See traveler E070310 for actuators: 1. check for and remove any visible large particles between coil and magnet with plastic tweezers or methanol spray, 2. ultrasonic in methanol for 10 minutes or spray out gaps and holes with methanol if ultrasonic cleaner is insufficient, 3. let dry under a heat lamp for 24 hours or until all gaps, holes or tight areas have had a chance to dry out, 4. vacuum bake at 150C for 48 hours.

See traveler E070328 for the capacitive position sensors: 1. ultrasonic clean in methanol for 10 minutes, 2. Soak in isopropyl alcohol for 10 minutes agitating regularly 3. Vacuum bake at 100C for 48 hours.

Vacuum pods for the Trillium, GS-13 and L4-C seismometers will be cleaned and baked before the insertion of the instruments. The vacuum pods are then filled with a neon tracer gas for leak detection.

It is as yet unclear if the tracking of the clean and bake of parts will be done using cleaning travelers as in the past or whether this will be replaced by the new JIRA inventory control system. This is a systems level decision rather than an SEI level decision.

7.2 Leak checking

Each BSC-ISI platform utilizes 6 L4-C sensors, 6 GS-13 sensors and 3 Trillium T-240 sensors. These sensors are enclosed in vacuum sealed pods prior to being mounted on the platform. This maintains system cleanliness while allowing the sensors to operate in an environment at atmospheric pressure.

One of our main concerns is with contamination of the vacuum due to a leak in one of the vacuum pods. In T0900192 we outline the basis for these concerns and conclude that we have to adopt a zero-tolerance approach with respect to leaks. This is mainly driven by the GS-13 instrument which uses several substances in its construction which are inimical to our vacuum (e.g. machine oil). Each sensor will be huddle tested prior to being installed in a vacuum pod. During assembly the pod is filled with at least 0.1 atmospheres of Neon gas. This gas is used to identify leaks after assembly. We leak test the pods in a vacuum oven and are sensitive to leak rates on the order of 1e-9 torr-liters/s. All pods will be assembled at the Livingston site. Pods which are shipped to Hanford will be leak-tested at Hanford prior to installation on an ISI platform. After leak-testing care will be taken to ensure that the pods endure no rough handling that might cause a leak. We are also investigating the use of a more robust vacuum feed-through. Our current feed-throughs come from Accuglass and there have been a couple of reported cases of leaks due to bent pins on the connectors. The new feed-through comes from SRI Hermetics (www.srihermetics.com). Preliminary indications are that these connectors are less susceptible to damage from baking and repeated cabling and uncabling.

Assembly documents exist for the L4-C (T080261) and the GS-13 (T080086) based on our experience in assembling and testing for the BSC-ISI prototype at LASTI and for the HAM-ISI platforms in use in the L1 and H1 interferometers. The BSC-ISI prototype uses STS-2 seismometers, but we intend to use Trillium T-240 seismometers in the production units. This will necessitate generating another assembly procedure.
It is worth noting that two of the sensor types on the current BSC-ISI prototype utilize motors to lock and unlock their masses. The T-240 does not require locking and will be simpler to install in a pod as a consequence. Thanks to research at Stanford we are also able to dispense with locking motors for the GS-13 instruments.

7.3 Assembly

The assembly procedure of the prototype is detailed in the document, E070347-00-D Advanced LIGO BSC ISI Assembly Procedure. This document will be fully updated along with the final design.

7.4 Storage

Once assembly and testing is complete the BSC ISI will be prepared per LIGO document E960022-B and placed in a modular container similar to the container designed for the HAM ISI (fig 114).

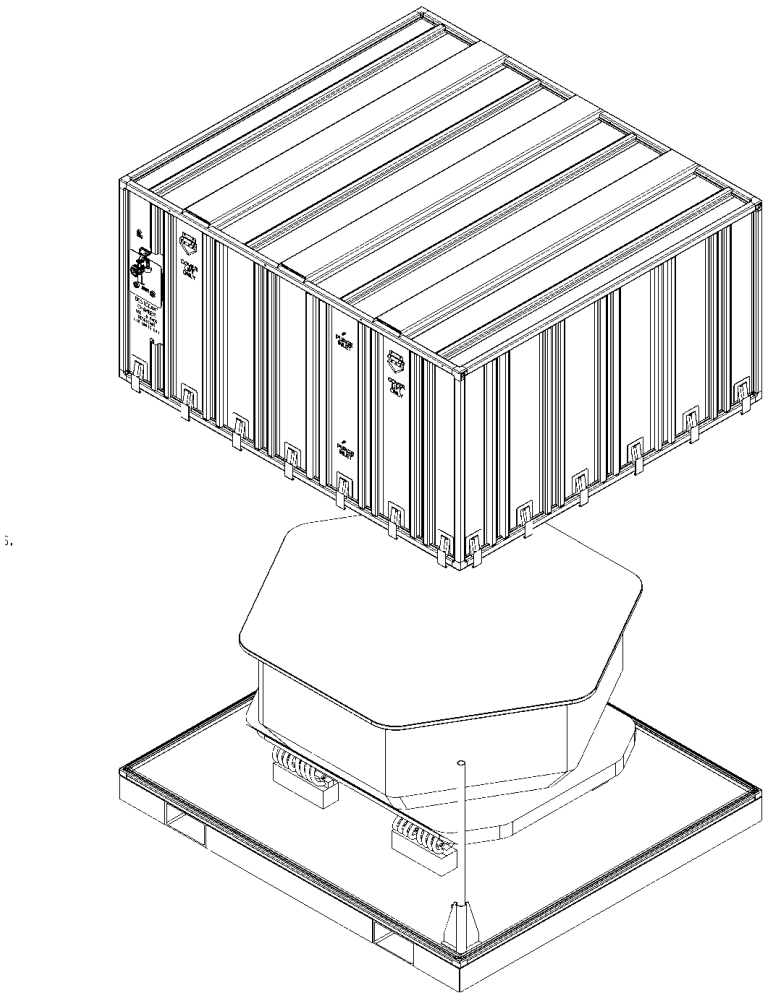

Figure 114: HAM ISI Shipping and Storage Container

This storage container consists of a steel pallet, mounting feet, and a sealed aluminum cover. The pallet is designed for a 10,000 lb load with fork lift guides sized for the RICO model PWH-100 pallet truck available at each of the sites. Since we will not be shipping fully assembled BSC isolation systems the mounting to the pallet will be on solid blocks without shock isolation. The lockers will be adequate for transporting the unit between the assembly area, warehouse, corner, and end stations. A continuous neoprene seal is in the pallet to allow purging of the storage container with dry nitrogen gas.
The cover is designed and tested to .25 psi. It includes a purge inlet and outlet port, humidity indicator, pressure relief valve, handles for lifting, and latches. The BSC ISI will be stored in clean warehouse space at each of the facilities. LIGO document D0810022-v1 is a floor plan of the LHO warehouse with floor space allocated for long term storage. A plan for monitoring the humidity during storage will be described in the FDR.

7.5 Installation

While still mounted on the test stand all three stages are locked together using the locator/lockers. A custom lifting attachment (D048048-A) is installed on top of the keel plate. The bolts holding stage zero onto the stand are removed.

At LASTI a BSC dome cover was then draped over the entire ISI. For aLIGO we will have a custom cover made. The clean room is then rolled out of the way and the crane is attached to the lifting ring. Using the crane the system is lifted ~1/2 inch and balanced if necessary (at LASTI no balancing was required). The isolation system will now be placed in the BSC chamber and bolted to the support tubes already installed.

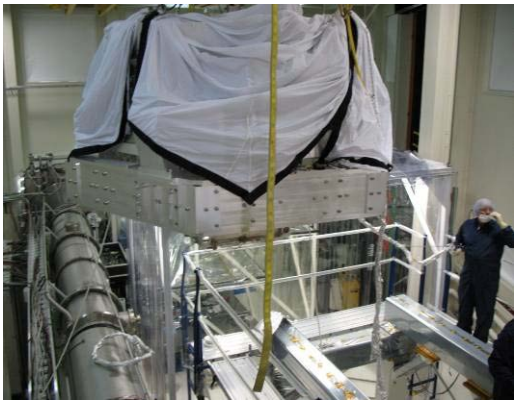

Figure 115

Figure 116

8 BSC-ISI Performances

8.1 Control Strategy

The feedback control approach is described on the diagram below. Stage 1 is instrumented with 6 Position Sensors (PS), 3 three-axis seismometers (STS for the prototype, Trilliums for Advanced LIGO) for the low frequency measurements and 6 single axis seismometers (L4C) for the high frequency measurements. Stage 2 is instrumented with 6 Position Sensors (PS), and 6 single axis seismometers (GS13). Although the motion of the stages are coupled to each other, the stages can be controlled independently as described in the next paragraph.

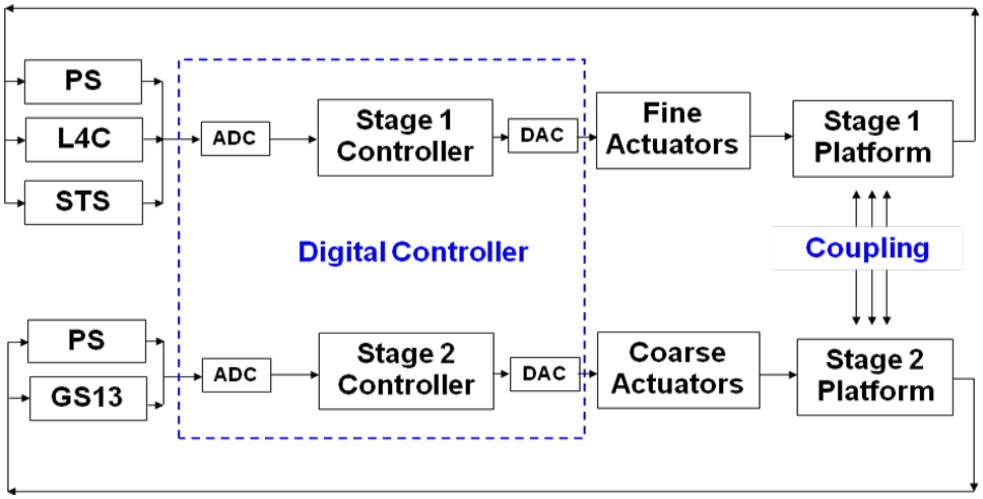

For each stage, the control is based on the use of 6 independent SISO loops. The control is done in the basis of the general coordinate system: X, Y, RZ, Z, RX, RY. X and Y are aligned with the arms of the interferometer. The position sensors are used to measure the relative position of the stage in the direction to be controlled through the Local to General coordinate change of basis matrix (L2G on block 1of the diagram below). The same thing is done with the seismometer to get the inertial motion of the stage in the direction to be controlled in the general basis.

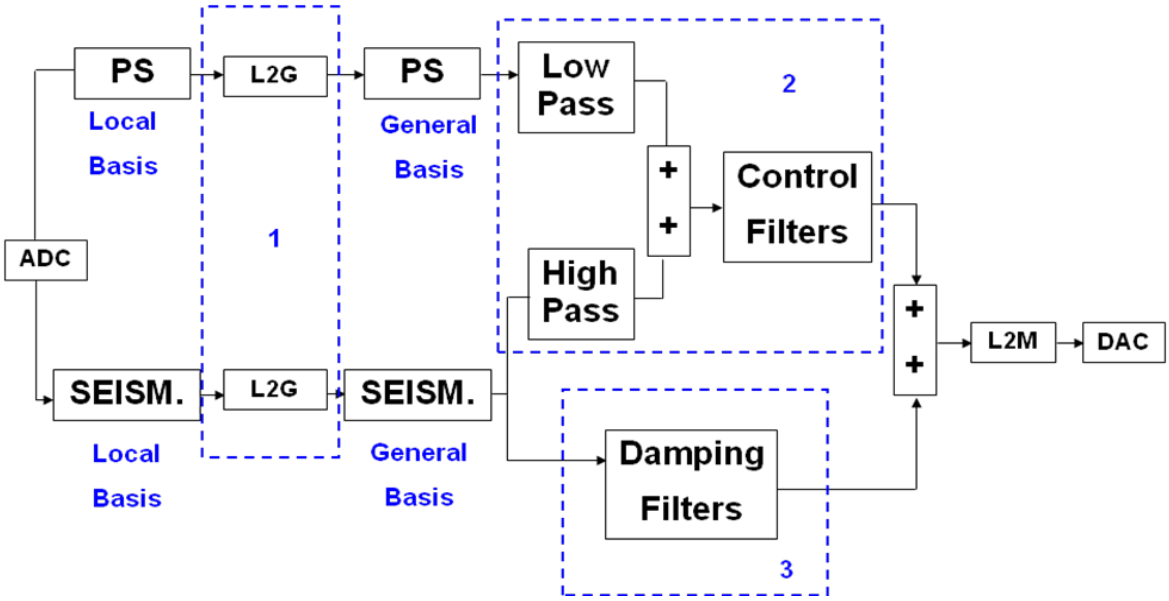

The seismometer signal sensors are first used to damp the suspension resonances (block 3 on the diagram above). Complementary filters are then used to blend the position sensors and the seismometers. The position sensors signal is filtered by the low pass and the seismometer is filtered by the high pass. The two signals are summed resulting in a super sensor (block 2 on the diagram above).

Finally a control filter is applied to the super-sensor to provide loop gain. Those filters typically set the unit gain frequency between 20Hz and 30Hz and the phase margin to 30 degrees. The control steps are detailed in document LIGO-T0900250, BSC-ISI Second Commissioning at LASTI.

8.2 Performance

- **Active control isolation**

The plot below shows the motion of the optical table measured in the X direction with the GS13. The black curve shows the motion of the table when the control is off. The Blue curve shows the motion of the table with a high frequency blend on both stages. Position sensors and seismometers are blended at 0.7Hz and the active control provide isolation from 1Hz to 20Hz.

Once the system is under control, the "X to Ry" and "Y to Rx" motions are decoupled using a tilt decoupling matrix. Once this is done, the horizontal seismometers are less sensitive to tilt and the blend frequency can be lowered. For the red curve the blend frequency has been lowered to 0.2Hz on stage 2. The active control provides isolation from 0.25Hz to 20Hz.

For the purple curve, the sensor correction has been turned on. The principle of the sensor correction is to use the Stage1 inertial measurement (measured with STS) and to sum it up with Stage2 relative motion measured with capacitive position sensors.

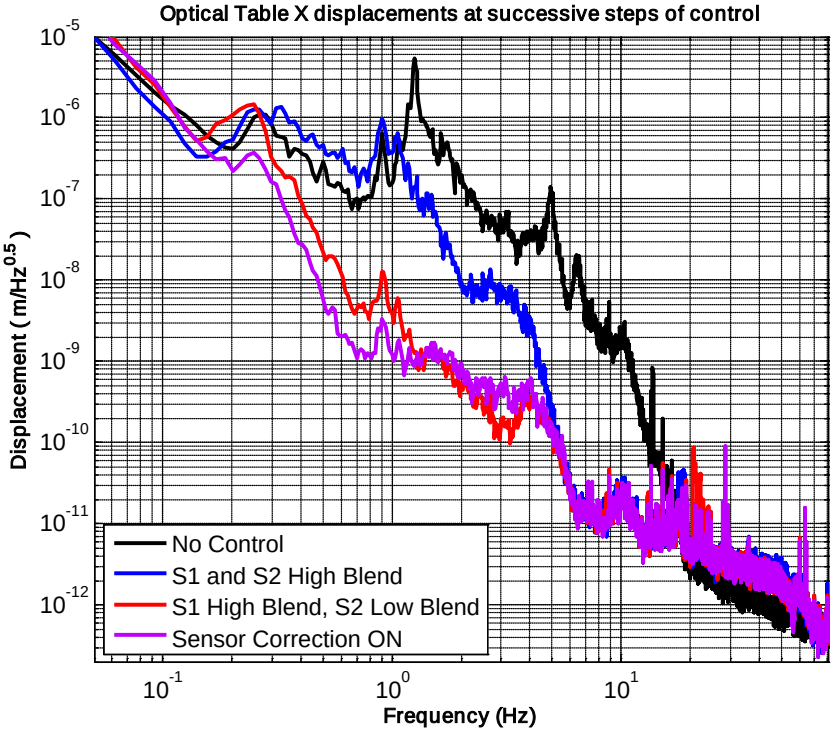

Figure 117

The next step will be to lower the blend frequency on stage1 which should provide the same level of improvement as from the blue curve to the red curve.

Although the stage 1 blend frequency has not been lowered yet, the current isolation matches expectations:

- At low frequencies (around 0.1Hz) there is very little motion amplification. This is where we usually are at risk to have gain peaking due to the use of a relative displacement signal in the sensors blend. In this case the sensor correction suppresses the gain peaking.

- The isolation starts as low as 0.1Hz which is good. It's usually hard to get isolation at lower frequencies due to the tilt sensitivity of the seismometers.

- The isolation at 1Hz is close to a factor of 100, which means that the position sensor is low passed with an average slope of 1/f^2, which is good. We could make it slightly more aggressive but it could result in a motion amplification at the blend frequency (0.1Hz).

- The control provides isolation up to 20Hz, which is good. The unit gain frequency is set up at 30Hz. The controller is quite aggressive in order to get a lot of gain at 10Hz. The drawbacks are a significant gain peaking above the unity gain frequency and nonexistent isolation between 20Hz and 30Hz. We think it's a good trade off since we need the ISI to provide a lot of active isolation at 10Hz but not much at 20Hz and above where the quadruple pendulum provides a lot of isolation.

The same steps have been followed in the Y direction and have provided similar performance as shown on the figure below.

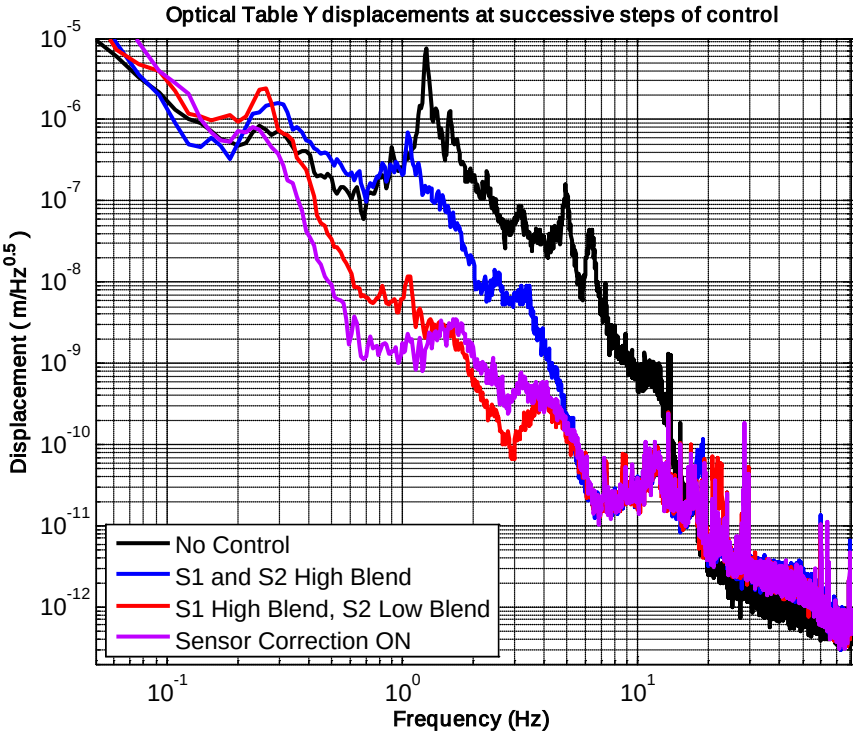

Figure 118

The same steps have been followed in the RZ direction and are presented on the figure below. The performance characteristics are comparable to those of stage X and Y except for the low frequency where the isolation starts only at 0.5Hz. There is also more gain peaking at 0.25Hz. The reason why the performance in the RZ direction is not quite as good as in X and Y is mostly because less time has been spent on it to improve its performance. This is on the list of next things to be done.

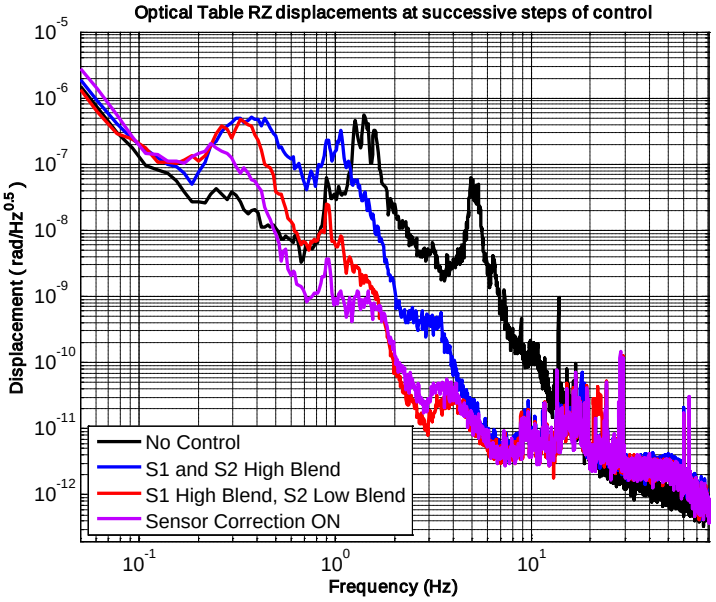

Figure 119

The Z control loop is the one showing the best performance. This is because it has a weaker coupling with the other degree of freedoms at high frequencies and it is less sensitive to tilt coupling at low frequencies. Therefore it provides a factor of isolation of 100 at 1Hz and 10Hz. On the figure below the isolation was however disappointing at 3Hz, which has been fixed since, by adjusting the controller to improve the performances at this frequency. The motion after control adjustment can be seen later on.

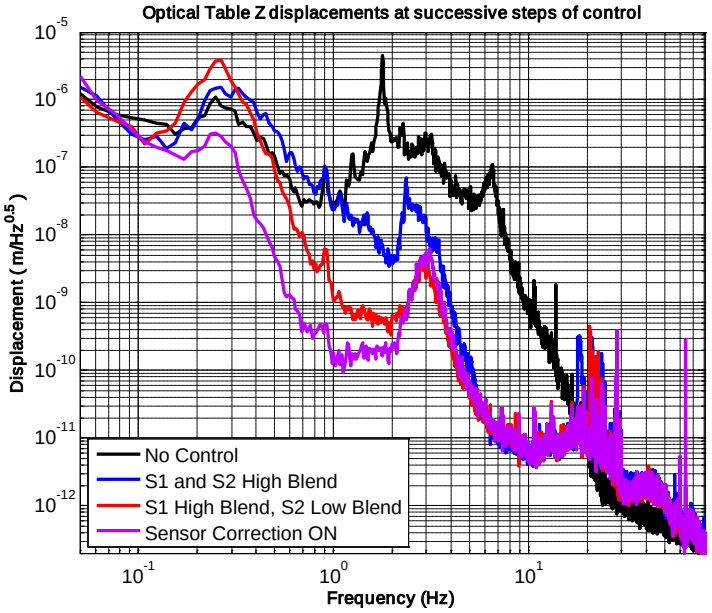

Figure 120

RX control performance is shown on the plot below. The isolation characteristic are similar to the other directions previously described except for the low frequency. In this case the blend frequency is set up at 0.4Hz which is why we don't have isolation above 0.5Hz. The reason why the blend frequency is set up higher on RX is to reduce the low frequency gain peaking and consequently the tilt motion amplification that would couple with the control of the horizontal degrees of freedom.

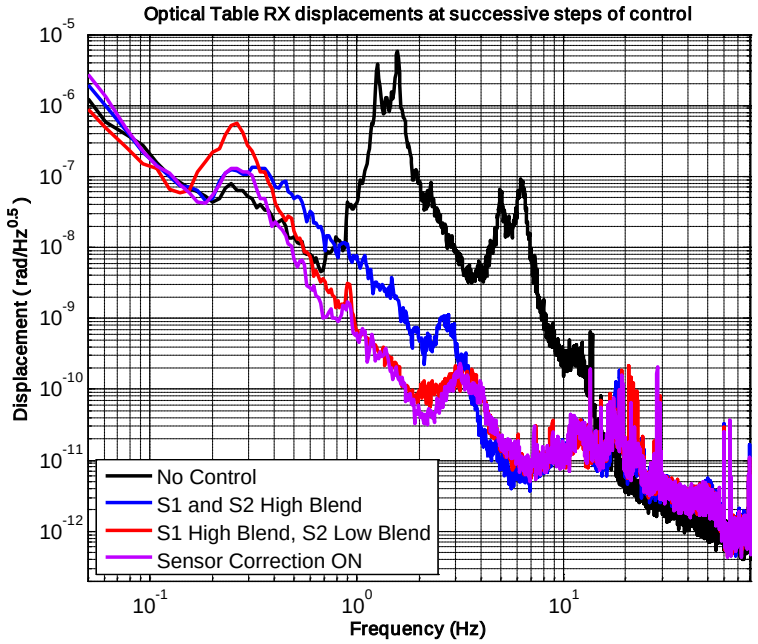

Figure 121

Ry control and performance characteristic are very similar to those of Rx. They are shown on the figure below.

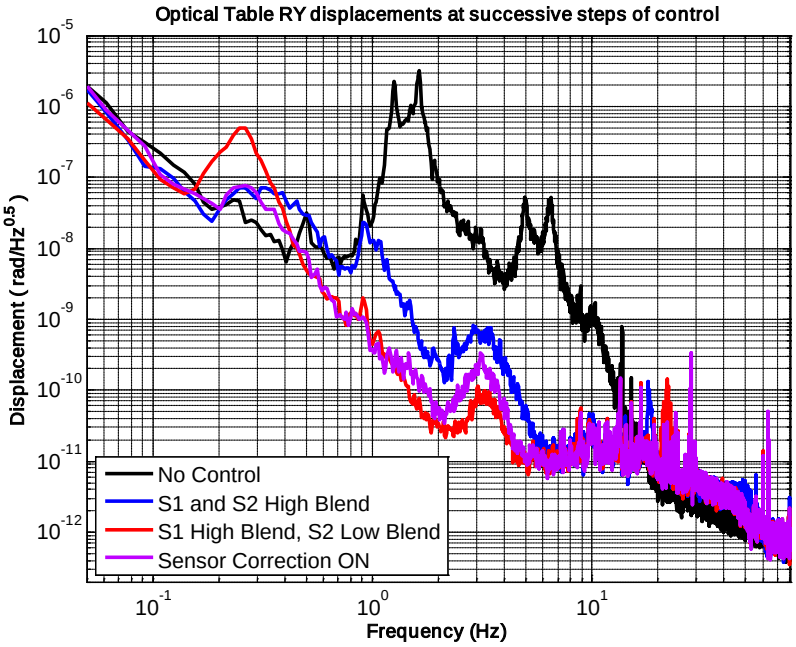

Figure 122

- **Global isolation (Active & Passive).**

The previous section presented the control performance (motion of the optical table with control on versus motion of the optical table with control off). In this section we compare the motion of the ground, the motion at the top of the HEPI piers, the motion of the optical table control off, the motion of the optical table control on, and the requirements.

The requirements curve is based on Advanced LIGO requirements and have been normalized as follows: AdL requirements (E990303, p.7) divided by the typical motion at LLO (E990303, p.3) and multiplied by the ground motion at MIT.

Only the translation global performance is presented since we don't have yet a rotation measurement of the ground nor a good calibrated rotation data of the HEPI piers.

On all of the plots below the HEPI system is not operating. It will provide an extra factor of isolation when it will be turned on. We are currently working on restoring HEPI control.

On the following plots:

- The ground motion is shown in Black. It is measured with a STS seismometers sitting on the ground 20 feet away from the BSC chamber.

- The HEPI motion is shown in Blue. It is measured with HEPI L4Cs.

- The motion of stage2 when the control is off is presented in Red

- The motion of stage2 when the control is on is presented in Purple

- The relative requirements are presented in Grey

The performances in the X direction are presented on the figure below. The comparison of the blue curve with the black curve shows how the motion at the top of the HEPI piers is amplified around 10Hz. We believe this amplification is both due to the modes of the piers but more importantly to the tilt of the chamber that is big enough to rock the ground.
The Red curve shows the motion of the optical table when the active control is off. It provides passive isolation with a factor of 100 at 10Hz and 800 at 20Hz. The motion of the optical table when the control is on is shown in purple. The system provides a total factor of isolation of 6800 at 10Hz.

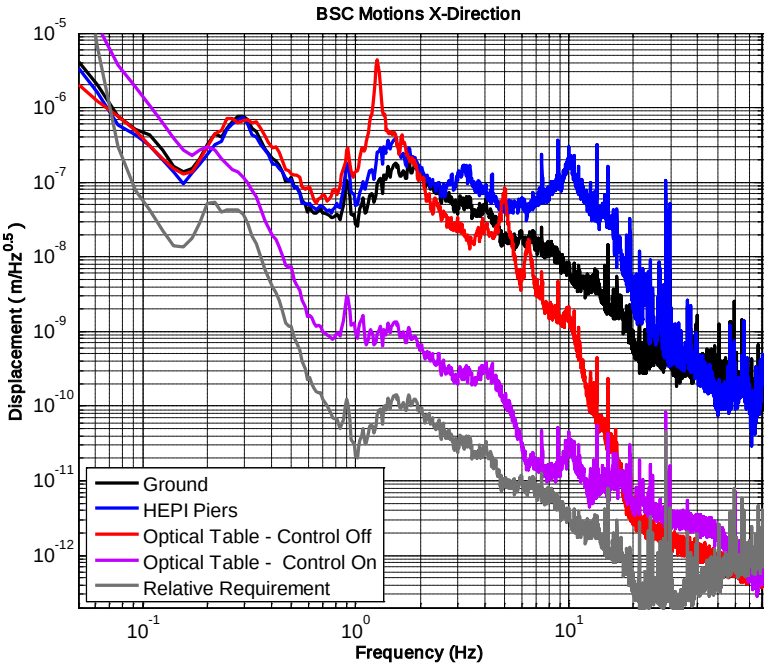

Figure 123

The HEPI control and the lower frequency blend that is going to be used on Stage1 should help to meet the requirements from 0.2Hz to about 8Hz. The sensor correction from stage1 to stage 2 will be adjusted in order to improve the performances around 0.1Hz. Above 10Hz it will be difficult to meet the initial requirements. This is not because the BSC-ISI doesn't meet the performance expected by design. It's because the motion at the top of the piers may have been under-estimated. The consequences of not meeting the requirements above 10Hz is discusses in the next paragraph.

The performances in the Y direction is presented on the plot below. The motion characteristics at all the stages are very similar to those of X. HEPI and stage1 lower frequency blend should help meeting requirements below 8Hz. Above 10 Hz the requirements will be hard to meet due to the excessive HEPI piers amplification.

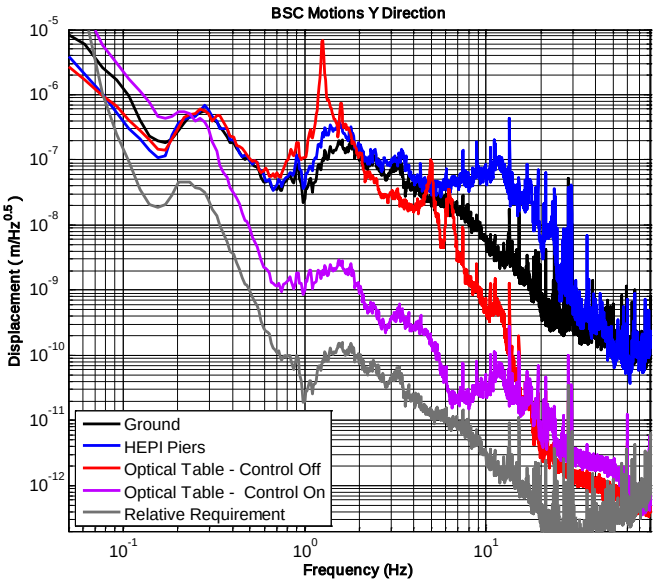

Figure 124

The performances in the Z direction are presented on the plot below.

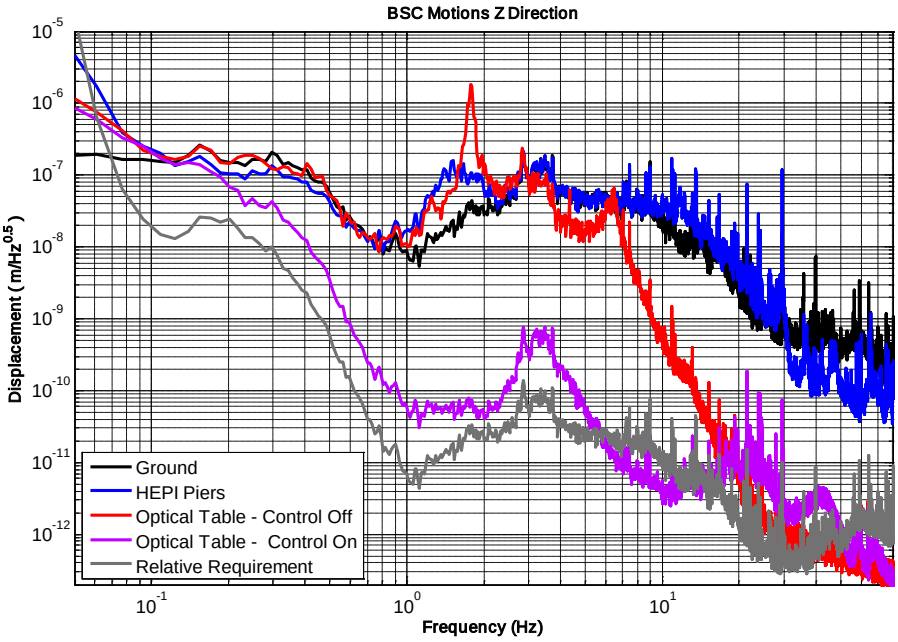

Figure 125

The HEPI control and stage1 lower frequency blend should help meeting requirements up to 16Hz in the Z direction.

- **Noise budget and perspective**

A predictive noise budget for Advanced LIGO has been presented in the document G0810021-v1, Some Advanced LIGO Systems Topics. At 17Hz the seismic noise was below the other sources of noise as shown on the plot below.

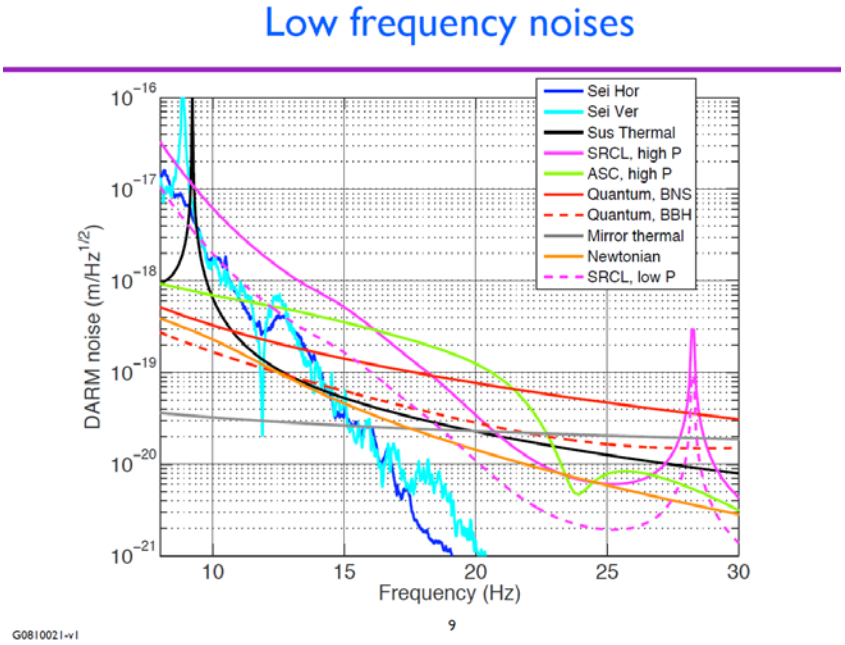

Figure 126

And this noise estimation was based on the BSC-ISI performances as of November 2008. This performance has been improved since as shown on the plot below:

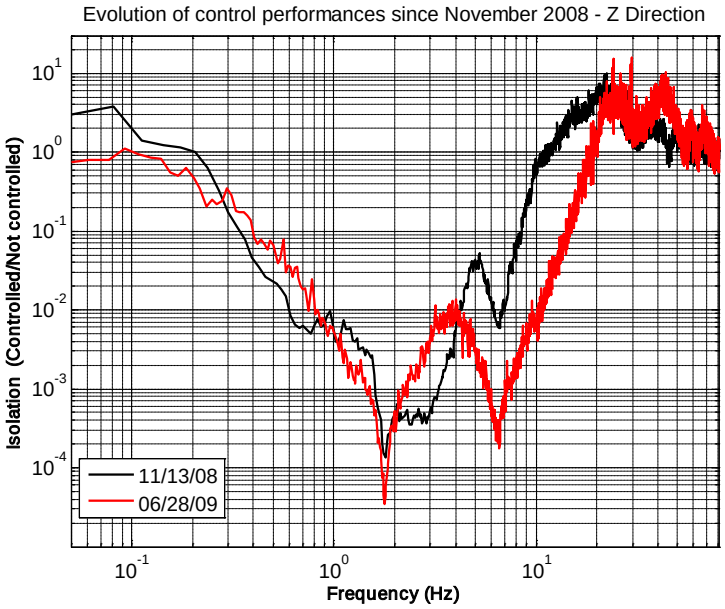

Figure 127

Although the initial requirements defined in E0300179 won't necessarily be met above 10Hz because of the HEPI piers motion amplification, we believe that the BSC-ISI provide satisfactory isolation to compensate this problem and maintain the seismic noise sufficiently below the other source of noise. Complementary feedforward approaches will be tested to improve the performance at those frequencies as described in next section.

8.3 Next step and perspective

Control commissioning at LASTI

- Stage 1 blend frequency will be lowered
- HEPI feedback control will be restored
- Sensor correction from the Ground to HEPI will be implemented

Those steps have already been done in the past and have proven to significantly improve the performance.

Some other steps never tried before will also be tested:

- Sensor correction from HEPI L4C to Stage1
- Feedforward from HEPI to Stage1 at high frequencies (10Hz-20Hz)
- Feedforward from Stage1 to Stage2 at high frequencies (10Hz-20Hz)

Finally, L4Cs will be mounted on Stage 0 of the prototype and feedforward from Stage0 to Stage1 will be tried. This could be the most efficient feedforward approach since:

- the path is more direct than from HEPI to Stage1. It should include less signal due to local deformations and should consequently be more efficient.
- the source of feedforward is well decoupled from the action which is not true for a feedforward from stage 1 to stage2.

9 Schedule Milestones and Early Procurements

9.1 Schedule Highlights

SI-MA3270 SEI PD: BSC Seismic Isolation Prelim. Design Rev (PDR)	30-Jun-09 – 15-July-09
SI-D23312 EST: SEI FD BSC Mech. Design Update	15-Oct-09 - 28-Oct-09
SI-F02445E SEI FAB: RFQ thru Award BSC ISI Instruments	29-Oct-09 - 05-Feb-10
SI-F02445A SEI FAB: BSC ISI Instruments	03-May-10
SI-F02446D SEI FAB: RFQ thru Award BSC ISI Mechanics	29-Oct-09 - 05-Feb-10
F02446A SEI FAB: IFO1 BSC ISI Mechanics	08-Jul-10
SI-F02446B SEI FAB: IFO2 BSC ISI Mechanics	29-Jul-10
SI-F02446C SEI FAB: IFO3 BSC ISI Mechanics	14-Oct-10
SI-F02447D SEI FAB: RFQ thru Award BSC ISI Elect & Controls	29-Oct-09 - 05-Feb-10
SI-F02447A SEI FAB: IFO1 BSC ISI Electronics & Controls	18-Aug-10
SI-F02447B SEI FAB: IFO2 BSC ISI Electronics & Controls	30-Sep-10
SI-F02447C SEI FAB: IFO3 BSC ISI Electronics & Controls	11-Nov-10
SI-M7120 Two Stage Seismic Isolation Assembly Start	08-Jul-10
SI-F02448B SEI FAB: IFO1 BSC ISI Assembly NSF	08-Jul-10 - 08-Mar-11
SI-F02448A SEI FAB: IFO2 BSC ISI Assembly NSF	29-Jul-10 - 29-Mar-11
SI-F02448C SEI FAB: IFO3 BSC ISI Assembly NSF	18-Jan-11 11-Aug-11
SI-F02439A SEI FAB: BSC ISI/SUS 1st Article Cartridge Test	29-Oct-10 18-Nov-10
SI-F02449B SEI FAB: IFO1 BSC ISI Functional Checkout	08-Oct-10 29-Mar-11
SI-M7042 SEI FAB: BSC ISI Ready for IFO1 NSF	05-Apr-11
SI-F02449A SEI FAB: IFO2 BSC ISI Functional Checkout	29-Oct-10 19-Apr-
SI-M7032 SEI FAB: BSC ISI Ready for IFO2	26-Apr-11
SI-F02449C SEI FAB: IFO3 BSC ISI Functional Checkout	23-Mar-11 01-Sep-11
SI-M7052 SEI FAB: BSC ISI Ready for IFO3 NSF	09-Sep-11

9.2 Early Procurements:

The following procurements can be started early to help reduce the procurement and assembly time. The most important of these are the seismometer and pod assemblies. It takes considerable time to assemble the units in the pod, purge with neon gas, leak check, and test the pod assembly.

The following items are either complete or nearly complete and are candidates for early procurement:

Description	Proc,. ID	Status
GS-13 Seismometers	SI-165	Order Placed

GS-13 Pods	SI-193	Design inc. as part of this PDR – 7/30/09
L4-C Seismometers	SI-175	Ready for procurement
L4-C Pods	SI-193	Ready for Procurement
Trillium 240 OB Seismometer	SI-107b	Specs inc. as part of this review – 7/15/09
Trillium 240 OB Pods	SI-193	Design inc. as part of this PDR – 7/30/09
ADE Position Sensors	SI-162	Ready for Procurement
Large Electromagnetic Actuators	SI-170	Order Placed
Small Electromagnetic Actuators	SI-170	Design inc. as part of this PDR 8/30/09
In-vac Cabling	SI-164	Ready for Procurement
Actuator Coil Drivers	SI-300	Ready for Procurement
In pod wire harnesses	SI-165	Ready for Procurement

10 Remaining Steps to the FDR

10.1 Design

The Stage0, Stage1, Stage2, Actuators Brackets and Seismometers sub-projects are on time according to the re-design schedule M0900175-v1.

We are going to start the detailing phase for those project. Our objective is to have the drawings ready for the FDR.

We are behind schedule on the Flexure Rods sub-project. More manpower will be affected to this project to bring it back on time. As for the other subprojects, our objective is to have the drawings ready for the FDR.

We start working on the tooling re-design like it was schedule in M0900175-v1.

10.2 Testing

The shims on the prototype at LASTI will be adjusted to lower the amount of trim masses used on stage1. 500pds are currently use which results in concentrated masses creating local deformations.

10.3 Control

The control commissioning continues as described in section 8.3.

10.4 Documentation

The following documents must be prepared before the FDR:

- Assembly procedure and hazard analysis.

- Installation procedure and Hazard analysis.

- First article testing plan

11 PDR Check list M050220-09

1	System Design Requirements, especially any changes or refinements from DRR	**Mechanical: E030179-A** **Performances: E990303-03-D**
2	Subsystem and hardware requirements, and design approach	**BSC-CDR-ASI20008644-A** **Technical Memorandum: 20009033-A**
3	Justification that the design can satisfy the functional and performance requirements	**Section 8 of this document**
4	Subsystem block and functional diagrams	**p.48 of this document**
5	Equipment layouts	**Section 2 of this document for the initial design.** **Section 4 for the new design.**
6	Document tree and preliminary drawings (information issued)	**LIGO E050065-C for the drawings of the initial design.** **A new tree will be created for the drawings of the final design.** **Links to the rest of the documentation are posted on the Advanced LIGO wiki page**
7	Modeling, test, and simulation data	**Technical Memorandum: 20009033-A for the modeling and simulations.** **Section 3 & 8 of this document for testing.**
8	Thermal and/or mechanical stress aspects	**BSC-CDR-ASI 20008644-A** **Technical Memorandum: 20009033-A**
9	Vacuum aspects	**Actuators and ADE capacitive sensors passed RGA.** **Section 7 of this document for the seismometers pods leak test.**
10	Material considerations and selection	**All 7075 parts used in the initial design have been replaced by 2024-T4 in the final design.** **All other materials used are on the vacuum approved list.**
11	Environmental controls and thermal design aspects	**Thermal dissipation of the actuators T060076.**

12	Software and computational design aspects	**In the process of designing the control topology and the operator interface at LASTI**
13	Power distribution and grounding	**Electronics overview: D0901301-V1**
14	Electromagnetic compatibility considerations	**It will be measured at the next opening of the chamber in September 2009.**
15	Fault Detection, Isolation, & Recovery strategy	**The watch dog approach used for the HAM will be adjusted to the BSC**
16	Resolution to action items from DRR	**Section 4 of this document**
17	Interface control documents	**Per SEI requirements E990363-03**
18	Instrumentation, control, diagnostics design approach	**Instrumentation, control: Section 8 of this document.** **Diagnostics: TBD**
19	Fabrication and manufacturing considerations	**- Stage 0 design review** **- Stage 1 design review** **- Stage 2 design review**
20	Preliminary reliability/availability issues	**- Redundant mechanical protections for actuators and position sensors** **- Software watchdogs** **- L4C designed to be shipped unlocked** **- GS13 retrofitted with the new flexure rods. See section on sensors.** **- Moved from STS to Trilium which is 1.5 million hours mean time between failure. Expected to be better in our environment.** **- Working with the CDS on the reliability of the computer.**
21	Installation and integration plan	**Section 7.5 of this document.**
22	Environment, safety, and health issues	**Hazard analysis will be done for the FDR**
23	Mitigation of personnel and equipment safety hazards Reflected in equipment design and procedures for use	**Hazard analysis will be done for the FDR**
24	Human resource needs, cost and schedule	**Section 9 of this document**

25	Any long-lead procurements	**Section 9 of this document**
26	Technical, cost & schedule risks and planned mitigation	**AdL Risk register**
27	Test plan overview	**Schedule M0900175-v1**
28	Planned tests or identification of data to be analyzed to verify performance in prototyping phase	**Section 3 of this document**
30	In production/installation/integration phase	**Section 9 of this document**
31	Identification of testing resources	**TBD**
32	The test equipment required for each test adequately identified	**TBD**
33	Organizations/individuals to perform each test identified	**TBD**
34	QA involvement	**Mick Flanigan involved in procurement, inspection and testing**
35	Test and evaluation schedule, prototype and production	**Section 3 of this document. Production schedule**
36	Lessons learned documented, circulated	**Section 3 of this document.**
37	Problems and concerns	**Control and design issues addressed and under correction as described in this document.**